การสังเคราะห์โอเลโออิล-4-คาร์บอกซีเบนซีนซัลโฟนาไมด์-ควอเทอร์ไนซ์ไคโทซาน

นางสาวธารทิพย์ เดชอุดมสุทธิ์

วิทยานิพนธ์นี้เป็นส่วนหนึ่งของการศึกษาตามหลักสูตรปริญญาวิทยาศาสตรมหาบัณฑิต
สาขาวิชาปิโตรเคมีและวิทยาศาสตร์พอลิเมอร์
คณะวิทยาศาสตร์ จุฬาลงกรณ์มหาวิทยาลัย
ปีการศึกษา 2557
ลิขสิทธิ์ของจุฬาลงกรณ์มหาวิทยาลัย

SYNTHESIS OF OLEOYL-4-CARBOXYBENZENESULFONAMIDE-QUATERNIZED CHITOSAN

Miss Tanthip Detu-domsut

A Thesis Submitted in Partial Fulfillment of the Requirements

for the Degree of Master of Science Program in Petrochemistry and Polymer Science

Faculty of Science

Chulalongkorn University

Academic Year 2014

Thesis Title	SYNTHESIS OF OLEOYL-4-CARBOXYBENZENESULFONAMIDE-QUATERNIZED CHITOSAN
By	Miss Tanthip Detu-domsut
Field of Study	Petrochemistry and Polymer Science
Thesis Advisor	Associate Professor Nongnuj Muangsin, Ph.D.

Accepted by the Faculty of Science, Chulalongkorn University in Partial Fulfillment of the Requirements for the Master's Degree

....Dean of the Faculty of Science

(Professor Supot Hannongbua, Dr.rer.nat.)

THESIS COMMITTEE

....Chairman

(Professor Pattarapan Prasassarakich, Ph.D.)

....Thesis Advisor

(Associate Professor Nongnuj Muangsin, Ph.D.)

....Examiner

(Assistant Professor Anawat Ajavakom, Ph.D.)

....External Examiner

(Assistant Professor Nalena Praphairaksit, Ph.D.)

ธารทิพย์ เดชอุดมสุทธิ์ : การสังเคราะห์โอเลโออิล-4-คาร์บอกซีเบนซีนซัลโฟนาไมด์-ควอ
เทอร์ไนซ์ไคโทซาน (SYNTHESIS OF OLEOYL-4-CARBOXYBENZENESULFONAMIDE-
QUATERNIZED CHITOSAN) อ.ที่ปรึกษาวิทยานิพนธ์หลัก: รศ. ดร.นงนุช เหมืองสิน, 83
หน้า.

วัตถุประสงค์ของงานวิจัยนี้คือเพิ่มคุณสมบัติการยึดติดเยื่อเมือกของไคโทซานโดยการดัด
แปรและนำมาใช้เป็นพอลิเมอร์สำหรับระบบนำส่งยา ไคโทซานที่ถูกดัดแปรทั้งสองชนิดคือ โอเลโออิล-
4-คาร์บอกซีเบนซีนซัลโฟนาไมด์-ไตรเมทิลไคโทซานคลอไรด์ (OA-4-CBS-TMC) และโอเลโออิล-4-
คาร์บอกซีเบนซีนซัลโฟนาไมด์-ไคโทซาน 3-คลอโร-2-ไฮดรอกซีโพรพิลไตรเมทิลแอมโมเนียมคลอไรด์
(OA-4-CBS-CS Quat-188) ซึ่งทำได้สำเร็จโดยการดัดแปร ไคโทซานด้วย 4-คาร์บอกซีเบนซีนซัลโฟ
นาไมด์ (4-CBS) และกรดโอเลอิก (OA) คอนจูเกตกับไตรเมทิลไคโทซานคลอไรด์ (TMC) หรือไคโท
ซาน 3-คลอโร-2-ไฮดรอกซีโพรพิลไตรเมทิลแอมโมเนียมคลอไรด์ (CS Quat-188) โดยใช้ 1-ethyl-3-
(3-dimethylaminopropyl)carbodiimide hydrochloride (EDAC) เป็น coupling agent ดีกรีค
วอเทอร์ไนซ์เซชัน (%DQ) ของ TMC และ CS Quat-188 คือ 18.90% และ 24.05% ตามลำดับ
ดีกรีการแทนที่ (%DS) ของ 4-CBS บน TMC, 4-CBS บน CS Quat-188, OA บน 4-CBS-TMC, และ
OA บน 4-CBS-CS Quat-188 คือ 9.70%, 10.36%, 34.15%, และ 37.88%, ตามลำดับ ซึ่งคำนวณ
โดยเทคนิค ^{1}H NMR ศึกษาความสามารถในการยึดติดเยื่อเมือกของพอลิเมอร์ที่ทดสอบด้วย Periodic
Acid Schiff (PAS) ในของเหลวจำลองระบบทางเดินอาหาร (pH 1.2 and 6.4) พบว่า OA-4-CBS-
TMC และ OA-4-CBS-CS Quat-188 ให้ความสามารถในการยึดติดเยื่อเมือก 2.60, 3.05, 1.48, และ
1.80 เท่า เมื่อเทียบกับไคโทซานที่ไม่ได้ดัดแปร ที่ pH 1.2 และ ที่ pH 6.4 ตามลำดับ สำหรับ fractal
hyperbranch ระดับนาโนเมตรของ OA-4-CBS-TMC และ OA-4-CBS-CS Quat-188 ที่ถูกเตรียม
ขึ้นด้วยเทคนิค self-assembly เนื่องจากเป็นวิธีที่ง่ายและมีความคงตัวโดยการ re-dispersing พอลิ
เมอร์ที่ถูกสังเคราะห์ขึ้นในน้ำที่ระดับความเข้มข้น 2.3 มิลลิกรัมต่อมิลลิลิตร พบว่าfractal
hyperbranch ระดับนาโนเมตรที่ถูกเตรียมได้มีการกระจายตัวทางความกว้างที่ค่อนข้างต่ำและมี
ขนาดเส้นผ่านศูนย์กลาง 2-9 ไมโครเมตร ดังนั้น OA-4-CBS-TMC และ OA-4-CBS-CS Quat-188
จึงมีความเหมาะสมที่จะนำไปใช้ในระบบนำส่งยาในสภาวะเลียนแบบระบบทางเดินอาหาร

สาขาวิชา   ปิโตรเคมีและวิทยาศาสตร์พอลิเมอร์ ลายมือชื่อนิสิต ....
ปีการศึกษา 2557   ลายมือชื่อ อ.ที่ปรึกษาหลัก ....

5571999523 : MAJOR PETROCHEMISTRY AND POLYMER SCIENCE

KEYWORDS: CHITOSAN / MUCOADHESIVE / SELF-ASSEMBLY

TANTHIP DETU-DOMSUT: SYNTHESIS OF OLEOYL-4-CARBOXYBENZENESULFONAMIDE-QUATERNIZED CHITOSAN. ADVISOR: ASSOC. PROF. NONGNUJ MUANGSIN, Ph.D., 83 pp.

The objectives of this research were to increase mucoadhesive properties of chitosan and then evaluate for using as mucoadhesive drug carrier. Two mucoadhesive modified chitosans, oleoyl-4-carboxybenzenesulfonamide-*N*-trimethyl chitosan chloride (OA-4-CBS-TMC), and oleoyl-4-carboxybenzenesulfonamide-chitosan *N*-(3-chloro-2-hydroxy-propyl) trimethylammonium chloride (OA-4-CBS-CS Quat-188), can be achieved by modification of chitosan with 4-CBS and OA conjugated with TMC or CS Quat-188 using 1-ethyl-3-(3-dimethylaminopropyl) carbodiimide hydrochloride (EDAC) as a coupling agent. The degree of quaternization (%DQ) of TMC and CS Qaut-188 were 18.90% and 24.05%, respectively. The degree of substitution (%DS) of 4-CBS on TMC, 4-CBS on CS Quat-188, OA on 4-CBS-TMC, and OA on 4-CBS-CS Quat-188 were 9.70%, 10.36%, 34.15%, and 37.88%, respectively which calculated by ^{1}H NMR. Periodic Acid Schiff (PAS) colorimetric method was used to study mucin-conjugated polymer bioadhesive strength in the simulated gastrointestinal fluid (pH 1.2 and 6.4). The OA-4-CBS-TMC and OA-4-CBS-CS Quat-188 showed stronger mucoadhesive properties 2.60, 3.05, 1.48, and 1.80-fold than that of unmodified chitosan at pH 1.2 and at pH 6.4, respectively. An easy and stable one step was presented to fabricate self-assembled well-ordered OA-4-CBS-TMC and OA-4-CBS-CS Quat-188 nanofractal hyperbranch. Nanofractal hyperbranch was prepared by only re-dispersing the polymeric compound in distilled water at a concentration of 2.3 mg/mL. The self-assembled nanofractal hyperbranch had diameter in the range of 2-9 µm with a narrow width distribution. Therefore, both OA-4-CBS-TMC and OA-4-CBS-CS Quat-188 could be suitable to use in gastrointestinal tract.

Field of Study:	Petrochemistry and	Student's Signature	....
	Polymer Science	Advisor's Signature	....
Academic Year:	2014		

ACKNOWLEDGEMENTS

CONTENTS

LIST OF TABLES

LIST OF FIGURES

LIST OF ABBREVIATIONS

%	Percentage
λ	Wavelength (lambda)
μL	Microliter
cm	Centimeter
CS	Chitosan
cm^{-1}	Wavenumber (unit)
4-CBS	4-Carboxybenzenesulfonamide
CS Quat-188	Chitosan *N*-(3-chloro-2-hydroxy-propyl)trimethylammonium chloride
°C	Degree Celsius
$\%DQ_{QCS}$	Degree of chitosan quaternization
$\%DS_{chitin}$	Degree of chitin substitution
$\%DS_{chitosan}$	Degree of chitosan substitution
$\%DS_{4\text{-}CBS}$	Degree of 4-carboxybenzenesulfonamide substitution
$\%DS_{OA}$	Degree of oleoyl chloride substitution
EDAC	1-Ethyl-3-(3-dimethylaminopropyl) carbodiimide hydrochloride

FT-IR	Fourier transformed infrared spectroscopy
g	gram
H	Hour
^{1}H NMR	^{1}H Nuclear Magnetic Resonance spectroscopy
kDa	Kilodalton
kV	Kilovolt
mA	Milliamps
mg	Milligram
mL	Milliliter
M	Molarity
MW	Molecular weight
μm	Micrometer
N	Normality
NHS	*N*-hydroxysuccinimide
NMP	*N*-methyl pyrolidone
nm	Nanometer
OA	Oleic acid
PAS	Periodic Acid Schiff

pH	A measure of the acidity or basicity of an aqueous solution
pK_a	Acid dissociation constant
QCS	Quaternized chitosan
rpm	Revolutions per minute
SEM	Scanning electron microscope
SD	Standard deviation
SGF	Simulated gastric fluid
SIF	Simulated intestinal fluid
TMC	*N*-Trimethyl chitosan chloride
UV-VIS	Ultraviolet-visible spectroscopy
v/v	Volume/volume
w/v	Weight/volume
w/w	Weight/weight

CHAPTER I

INTRODUCTION

1.1 Introduction

Nowadays, mucoadhesive polymers are increasing interest as excipients for drug delivery systems due to their several advantages, for example, their increased specificity and localization at the target site, a prolonged residence time at the site of required drug absorption that shows sustained release of drug there. The drugs absorbed through the mucosal lining of tissues can enter directly into the blood stream and not be inactivated by enzymatic degradation in the gastrointestinal tract and increase in drug concentration gradient on the mucosa, as a result, the bio-availability of drug can be improved. Due to these advantages, many attempts have been made to improve the mucoadhesive properties of polymeric carriers [1-4].

The mucoadhesive ability of any given compounds and dosage required are dependent upon a variety of factors, including the nature of the mucosal tissue containing the mucin glycoproteins of exceptionally high molecular weight having rich of sialic acid and sulphate groups content and thus mucous membrane behaving as an anionic polyelectrolyte [5, 6]. Another factor is physicochemical properties of the mucoadhesive polymers for adhesion with mucous membrane including strong hydrogen bonding group (carboxyl (-COOH) and hydroxyl (-OH) group), strong ionic charges (hydroxyl (-OH) and amino (-NH$_2$) group), sufficient chain flexibility, and high molecular weight [7-9].

Chitosan (CS) (Figure 1.1b), a cationic natural linear polyaminosaccharide composed of randomly distributed (1 →4) linked *D*-glucosamine and *N*-acetyl-*D*-glucosamine units, is obtained by the partial deacetylation of chitin (Figure 1.1a) and found in the exoskeleton of crustaceans such as crab and shrimp. Chitosan was used for mucoadhesive polymer because it is a non-toxic, bioactivity, biodegradable, biocompatible, and good mechanical properties [10-13]. Chitosan has a pK_a value of 6.2-7.0 that can be soluble in dilute acidic solutions below pH 6.0 due to the quaternization of the amine groups, whereas chitosan has low solubility in neutral

and basic conditions [14]. As a result, chitosan has limitations in solubility at wide range of pH. The backbone of chitosan consists of hydroxyl (-OH), primary amino (-NH$_2$) groups, and cationic property which can be responsible via non-covalent bond such as hydrogen bonding and electrostatic interactions with sialic acid and sulphate groups of the mucous membrane, resulting in a good mucoadhesive property. Therefore, chitosan is considered to be suitable for medicine applications such as drug and gene delivery carriers, tissue engineering scaffolds, and wound healing accelerators [15-20].
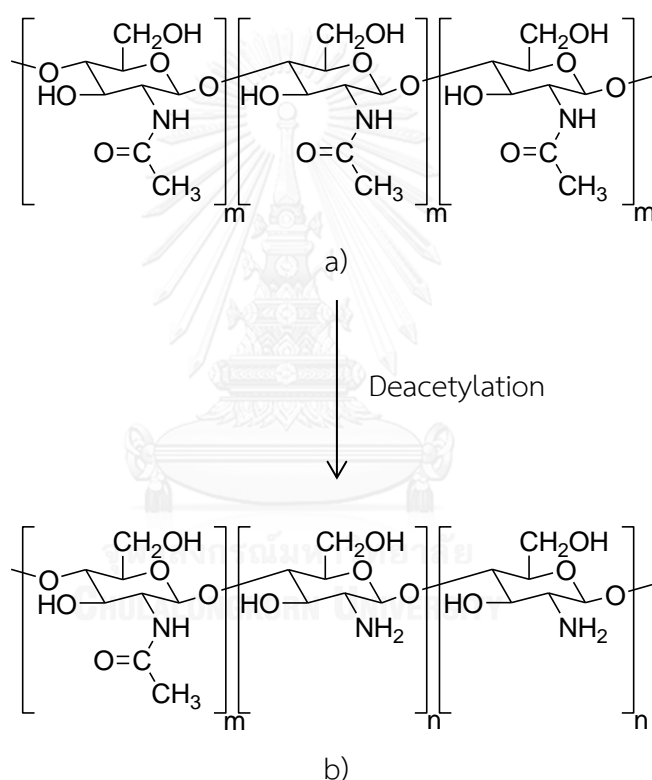
Figure 1.1 Structures of a) chitin and b) chitosan

Chitosan was quaternized to be *N*-trimethyl chitosan chloride (TMC) (Figure 1.2a) [14, 21-23] or chitosan *N*-(3-chloro-2-hydroxy-propyl)trimethylammonium chloride (CS Quat-188) (Figure 1.2b) [24] was increased permanently positive charges on chitosan. Quaternized chitosan (QCS) is a method to increase the solubility at wide range of pH and to improve the mucoadhesive properties of native chitosan which positive

charges on quaternized chitosan enhance electrostatic interaction with negative charges on mucin.

a)

b)
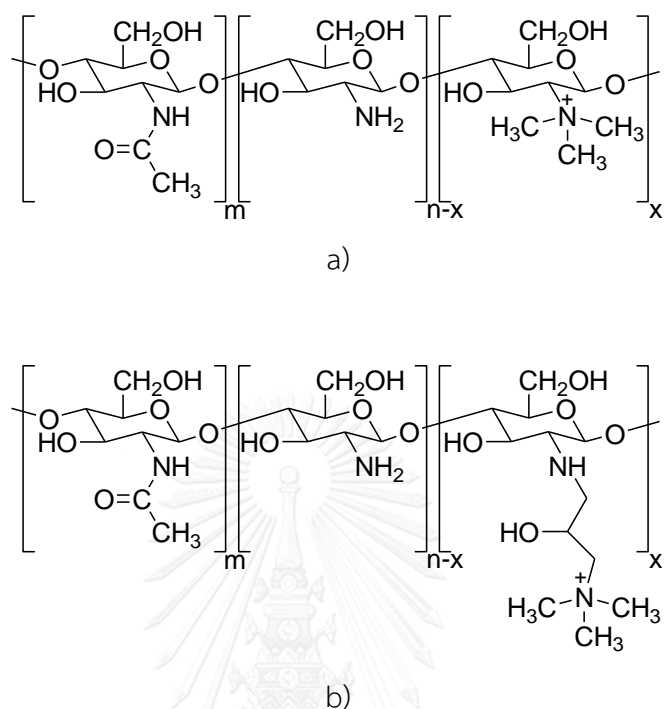
Figure 1.2 Structures of a) *N*-trimethyl chitosan chloride (TMC) and b) chitosan *N*-(3-chloro-2-hydroxy-propyl)trimethylammonium chloride (CS Quat-188)

Moreover, 4-carboxybenzenesulfonamide (4-CBS), aromatic sulfonamide groups, was used to modify chitosan to be mucoadhesive 4-carboxybenzenesulfonamide-chitosan (4-CBS-CS) (Figure 1.3). It exhibited 20-fold stronger mucoadhesive to mucin than native chitosan in the simulated gastric fluid (SGF; pH1.2) [25, 26].
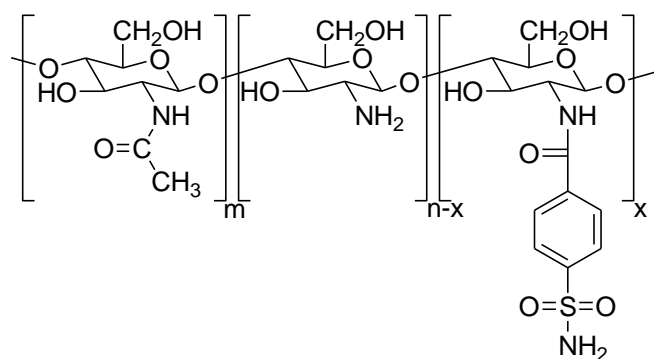
Figure 1.3 Structure of 4-carboxybenzenesulfonamide-chitosan (4-CBS-CS)

The aim of this study is to design and synthesize self-assembly mucoadhesive chitosan into various forms such as nanospheres, nanocubes, nanofractal hyperbranches, and other ordered structures for drug delivery system (as a model hydrophobic drugs) [27-30]. A typical self-assembly molecule contains two regions: a hydrophobic aliphatic tail such as oleic acid, cholesterol, linoleic acid, and stearic acid [31], and hydrophilic sequence attached to that tail. The electrostatic interaction, hydrophobic interaction, and hydrogen bonding have important roles on the morphology of self-assembly. These self-assembly mucoadhesive chitosan is designed in order to increase mucoadhesion and hydrophobicity. This can be performed by (i) increasing the positive charges on chitosan, (ii) conjugating aromatic sulfonamide group into the quaternized chitosan backbone to increase the mucoadhesive property and finally, (iii) conjugating long chain hydrocarbon to increase hydrophobicity for self-assembly micelles. This can be achieved by modification of chitosan with methyl iodide (CH_3I) or N-(3-chloro-2-hydroxy-propyl) trimethylammonium chloride (Quat-188) into quaternized chitosan (QCS) and conjugated with 4-carboxybenzene sulfonamide (4-CBS) and oleic acid (OA), respectively (Figure 1.4). The amount of positive charges quaternized on chitosan was determined by calculation from ^{1}H NMR, Periodic Acid Schiff (PAS) colorimetric method was used to qualify mucin-conjugated polymer bioadhesived strength in the simulated gastrointestinal fluid (pH 1.2 and 6.4).
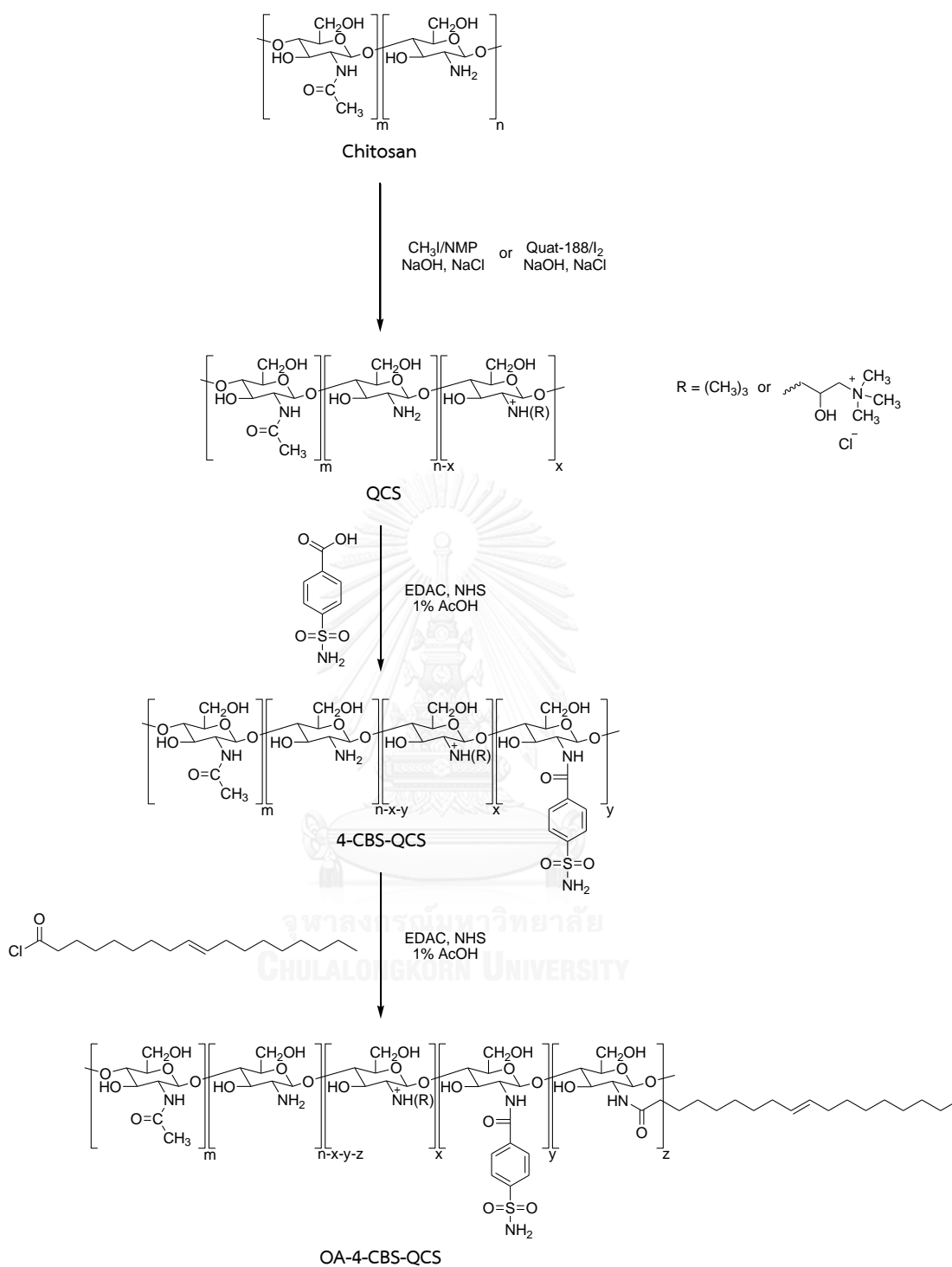
Figure 1.4 Synthesis scheme of oleoyl-4-carboxybenzenesulfonamide-quaternized chitosan (OA-4-CBS-QCS)

Therefore, to overcome the drawback of chitosan related with physical and chemical properties, and improved mucoadhesion, the self-assembled oleoyl-4-carboxybenzenesulfonamide-quaternized chitosan (OA-4-CBS-QCS) was prepared (Figure 1.5).
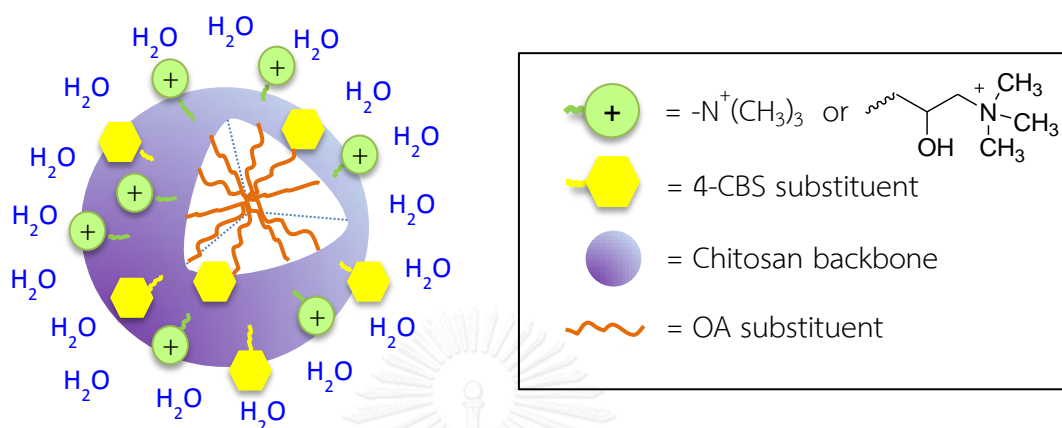
Figure 1.5 Scheme of the self-assembled mucoadhesive oleoyl-4-carboxybenzene sulfonamide-quaternized chitosan (OA-4-CBS-QCS) in distilled water.

1.2 The objectives of this research

1) Synthesize OA-4-CBS-QCS to improve mucoadhesive propoties suitable for hydrophobic drug delivery.

2) Design and fabricate OA-4-CBS-QCS mucoadhesive nanofractal hyperbranches based on the effect of re-dispersed concentration of polymer for using as drug carrier in acidic environment.

1.3 The scope of this research

The scope of this research was carried out by stepwise methodology as follows:

1) Review literature for related research work.

2) **Part I:** Modifying chitosan

    a. Preparation of *N*-trimethyl chitosan chloride (TMC), chitosan *N*-(3-chloro-2-hydroxy-propyl)trimethylammonium chloride (CS Quat-188), 4-carboxybenzenesulfonamide-*N*-trimethyl chitosan chloride (4-CBS-TMC), 4-carboxybenzenesulfonamide-chitosan *N*-(3-chloro-2-hydroxy-propyl)

trimethylammonium chloride (4-CBS-CS Quat-188), oleoyl-4-carboxybenzenesulfonamide-*N*-trimethyl chitosan chloride (OA-4-CBS-TMC), and oleoyl-4-carboxybenzenesulfonamide-chitosan *N*-(3-chloro-2-hydroxy-propyl)trimethylammonium chloride (OA-4-CBS-CS Quat-188).

b. Characterization of the physical and chemical properties of chitosan and modified chitosan using FT-IR and ^{1}H NMR.

c. Determination of the degree of quaternization of TMC and CS Quat-188 by using ^{1}H NMR.

d. Determination of the degree of 4-CBS and OA substitution by using ^{1}H NMR.

e. Determination of mucoadhesive properties of chitosan and modified chitosan in simulated gastric fluid (SGF, pH 1.2) and simulated intestinal fluid (SIF, pH 6.4) by the Periodic Acid Schiff (PAS) method.

f. Summary and discussion of the results.

Part II: Self-assembly mucoadhesive nanofractal hyperbranches

a. Fabrication and comparison self-assembled OA-4-CBS-TMC and OA-4-CBS-CS Quat-188 by re-dispersing the polymeric compound in distilled water with various concentration (0.3, 1.3, 2.3, 3.3, and 4.3 mg/ml) and studying the morphology and surface appearance of different concentration on self-assembly of OA-4-CBS-TMC and OA-4-CBS-CS Quat-188 particles by using SEM.

b. Summary and discussion of the results.

3) Report, discussion and thesis writing up.

CHAPTER II

THEORY AND LITERATURE REVIEWS

The cultural and economic pressures from humans seeking high quality of life and long lifespan have promoted the development of new strategies for the practice of medicine. This has coincided with, and likely promoted, the emergence of bionanotechnology. Applications of nanostructures from natural or synthetic molecules have been evaluated in disease diagnostics, drug delivery, tissue engineering, and regenerative.

The rapidly growing needs for new medical therapies continue to challenge the field of nanotechnology and nanoscience. The earliest examples of nanomedicines are essentially reformulations of existing drugs using nanostructured materials; however, the development of future medicines that could be more predictive, preemptive, personalized, and re-generative demands customized fabrication of nanostructures with properties specifically tailored for the desired medical propose. Consequently, they require a better structural and functional control of materials and drugs at the molecular level. This is where self-assembly can make a major contribution, allowing for the necessary control of bioactive architectures with adjustable sizes, shapes, and more importantly, surface chemistries, that can emulate three-dimensional structures of biological proteins.

2.1 Self-assembly

Self-assembly is a type of process in which a disordered system of pre-existing components forms an organize structure or pattern as a consequence of specific, local interactions among the components themselves, without external direction. When the constitutive components are molecules, the process is termed molecular self-assembly.

Self-assembly can be classified as either static or dynamic. In static self-assembly, the ordered state forms as a system approaches equilibrium, reducing its free energy. However in dynamic self-assembly, patterns of pre-existing components organized by

specific local interactions are not commonly described as self-assembled by scientists in the associated disciplines. These structures are better described as self-organized.

Macromolecular self-assembly presents a very attractive strategy to construct nanoscale materials due to its simplicity in application [32]. They were generated predominantly from DNA, peptides, proteins, lipids, copolymer, and dendrimers. They play a far more crucial role in governing the structures and functions of the entire body than any individual molecules [33].

Peptides may be the best candidate for self-assembly in medical application since they are major components in biological systems, their inherent biocompatibility and easy to synthesize using conventional technology. In particular, β-sheet-forming peptides demonstrate the extraordinary ability to assemble into one-dimensional nanostructures through intermolecular hydrogen bonding [34]. Interactions among one-dimensional peptide-based nanostructures can lead to the formation of three-dimensional networks. The chemical design versatility of peptide, in combination with their ability to adopt specific secondary structures, provides a unique platform for the design of materials with controllable structural features at the nanoscales. Additionally, the biodegradability, further tunable by incorporation of specific amino acid sequences or control over their self-assembled structures, allows for the construction of bioactive hydrogels that can mimic the structure and function of native extracellular matrix. The oligopeptides could serve as an effective, low-cost alternative for function mimicry of large proteins. The relationship of function and structure in natural proteins is pervasive, with the spatial organization provided by specific folding and residue interactions directly contributing to the functional activity. Through self-assembly, we hope to precisely combine functional peptide sequences with the versatile structure of self-assembling synthetic molecules to produce customized nanoscale engineered biomaterials for various medical applications.

2.2 Bioadhesion/Mucoadhesion

Bioadhesion defined any adhesive interaction formed between two biological surfaces such as platelet aggregation and wound healing or a bond between a biological and a synthetic surface such as cell adhesion to culture dishes and adhesion of synthetic hydrogels to soft tissues, which are held together for extended periods of time by interfacial forces [35, 36].

Mucoadhesion is the ability of macromolecules such as proteins and peptides to adhere at mucous membranes which are the moist surfaces lining the walls of various body cavities.

In the early 1980s, the concept of mucoadhesives, was introduced into the controlled drug delivery area. Mucoadhesives are synthetic or natural polymers that will attach to related tissue or to the surface coating of the tissue for targeting various absorptive mucosae such as ocular, nasal, oral routes, pulmonary, buccal, vaginal etc. The system of drug delivery is called as mucoadhesive drug delivery system. This system has several advantages such as [4];

1. Prolongs the residence time of the dosage form at the site of absorption for increasing drug absorption and bioavailability of drug.

2. Due to an increased residence time which it enhances absorption and hence increases the therapeutic efficacy of the drug.

3. High concentration gradient drug at the site of adhesion-absorption membrane which will create a driving force for the paracellular passive uptake.

4. Immediate absorption from the bioadhesive drug delivery system without previous dilution and possible degradation in luminal fluids of body.

5. Increase in drug bioavailability due to first pass metabolism avoidance.

6. Drug is protected from degradation in the acidic environment in the gastrointestinal tract.

7. Enhancement of topical action of certain drugs such as antibiotic against certain bacteria that colonize the stomach.

8. Improved patient compliance-ease of drug administration.

2.2.1 Mucous membrane

Mucous membranes (mucosae) are the moist surfaces lining the walls of various body cavities such as the gastrointestinal and respiratory tracts. They are viscosity gel layer that protects tissues and composed primarily of crosslinked and entangled mucin fibers secreted by goblet cells and submucosal gland [37, 38]. Mucous membrane consists of a connective tissue layer (the lamina propria) above which is an epithelial layer, the surface of which is made moist usually by the presence of a mucus layer. The epithelia may be either single layered (e.g. the stomach, small and large intestine, and bronchi) or multilayered/stratified (e.g. in the oesophagus, vagina, and cornea). The former contain goblet cells which secrete mucus directly onto the epithelial surfaces, the latter contain, or are adjacent to tissues containing, specialized glands such as salivary glands that secrete mucus onto the epithelial surface. Mucus is present as either a gel layer adherent to the mucous surface or as a luminal soluble or suspended form. The major components of all mucus gels are mucin glycoproteins which have pendant sialic acid and sulphate groups located on the glycoprotein molecules result in mucin behaving as an anionic polyelectrolyte at neutral pH, lysozyme, lactoferrin, lipids, polysaccharides, inorganic salts, various other ionic species, and water, the latter accounting for more than 95% of its weight, making it a highly hydrated system [6]. The mucin glycoproteins are the most important structure forming component of the mucus gel, resulting in its characteristic gel-like, cohesive and adhesive properties. The thickness of this mucus layer varies on different mucous surfaces, from 50 to 450 Am in the stomach [39, 40], to less than 1 Am in the oral cavity [41]. The major functions of mucus are that of protection and lubrication (they could be said to act as anti-adherents).
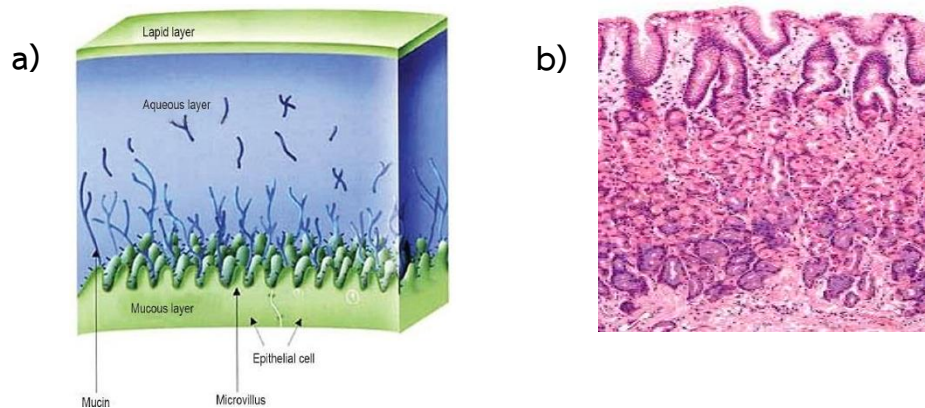
Figure 2.1 a) Mucous membrane structure and b) Histological section from the gastric antrum, showing the mucous of stomach.

2.2.2 Mucoadhesive mechanism

Development of novel mucoadhesive delivery systems are being undertaken so as to understand the various mechanism of mucoadhesion (Figure 2.2) and improved permeation of active agents.
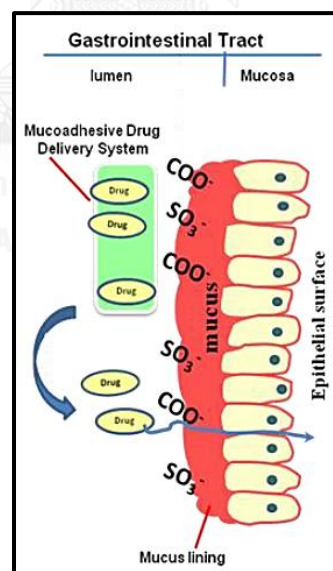
Figure 2.2 Mechanism of mucoadhesion

The mechanism of mucoadhesion is generally divided into two steps are shown in Figure 2.3 [4].

The first stage (also known as contact stage), the contact between the mucoadhesive polymer and mucous membrane, with spreading and swelling of the formulation, intiating its deep contact with the mucus layer.

The second stage (the consolidation stage), the mucoadhesive materials are activated by the presence of moisture. Moisture plasticizes the system, allowing the mucoadhesive molecules to break free and to link up by weak van der Waals and hydrogen bond
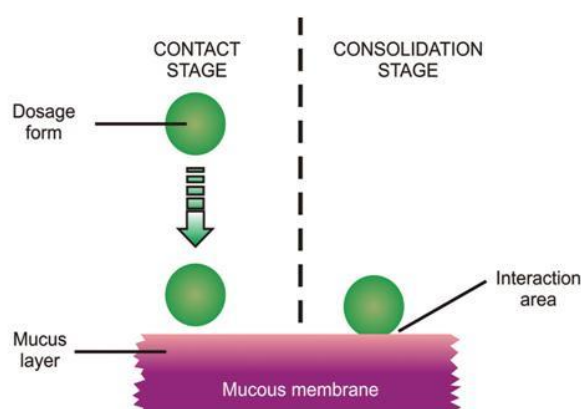
Figure 2.3 The two stages of the mucoadhesion process [42]

2.2.3 Mucoadhesion theories

There are six general theories have been proposed which can improve understanding for the phenomena of adhesion and can also be extended to explain the mechanism of bioadhesion [4, 42, 43]. However, each theoretical model can only explain a limited number of the diverse range of interactions which constitute the bioadhesive bond [44]. The theories include:

2.2.3.1 Electronic Theory

Electronic theory is based on the premise that both mucoadhesive and biological materials possess opposing electrical charges. Thus, when both materials come into contact, they transfer electrons leading to the building of a double electronic layer at the interface, where the attractive forces within this electronic double layer determines the mucoadhesive strength.

2.2.3.2 Wetting Theory

The wetting theory is the oldest established theory of adhesion applies to liquid or low-viscosity bioadhesive systems and considers surface and interfacial energies. It involves the ability of liquid to spread spontaneously onto a surface as a prerequisite for the development of adhesion. The affinity of a liquid for a surface can be found by using techniques such as the contact angle goniometry to measure the contact angel of the liquid on the surface, with the general rule being that the lower the contact angle then the greater the affinity of the liquid to the solid (Figure 2.4).
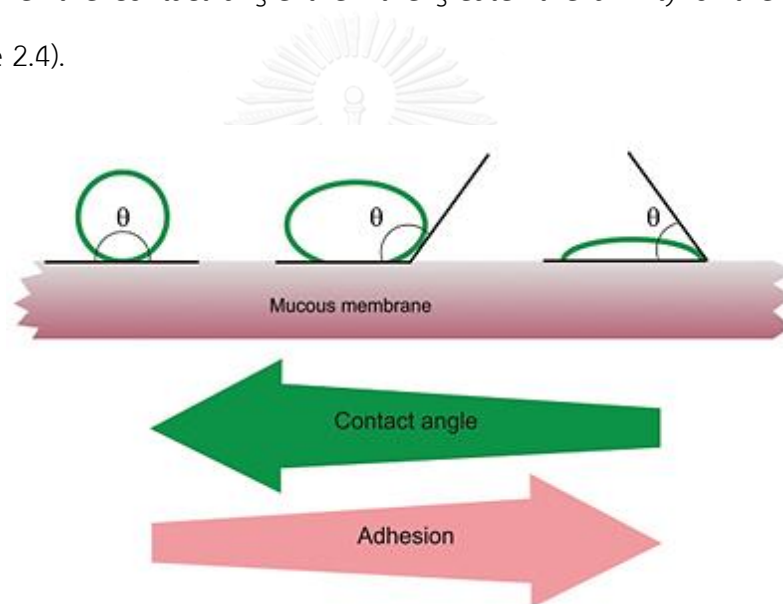
Figure 2.4 Schematic diagram showing influence of contact angle between device and mucous membrane on bioadhesion [42].

The spreading coefficient (S_{AB}) can be calculated from the surface energies of the solid and liquids using the equation:

$$S_{AB} = \gamma_B - \gamma_A - \gamma_{AB} \qquad \text{......(1)}$$

Where γ_A is the surface tension (energy) of the liquid A, γ_B is the surface energy of the solid B, and γ_{AB} is the interfacial energy between the solid and liquid. S_{AB} should be positive for the liquid to spread spontaneously over the solid.

The work of adhesion W_A represents the energy required to separate the two phases, and is given by:

$$W_A = \gamma_B + \gamma_A - \dot{\gamma}_{AB} \qquad ......(2)$$

The greater the individual surface energies of the solid and liquid relative to the interfacial energy, the greater the work of adhesion.

2.2.3.3 Adsorption Theory

According to the adsorption theory, the mucoadhesive device adheres to the mucus by secondary chemical interactions, such as van der Waals forces, hydrogen bonds, electrostatic attraction, and hydrophobic interactions [45]. For example, hydrogen bonds are the prevalent interfacial forces in polymers containing carboxyl groups. Such forces have been considered the most important in the adhesive interaction phenomenon, although they are individually weak, a great number of interactions can result in an intense global adhesion. A subsection of this, the chemisorption theory, assumes an interaction across the interface occurs as a result of strong covalent bonding.

2.2.3.4 Diffusion Theory

Interdiffusion of polymers chains is formed the bioadhesive interpenetrate into glycoprotein mucin chains across an adhesive interface shown in Figure 2.5 [46].
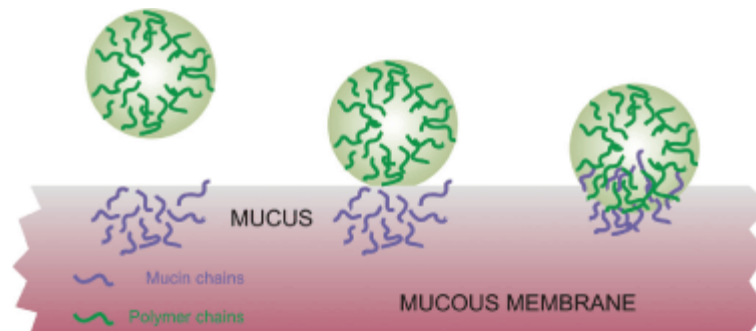
Figure 2.5 Secondary interactions resulting from interdiffusion of polymer chains of bioadhesive device and of mucus [42].

This process is driven by concentration gradients and is affected by the available molecular chain lengths and their mobilities. The depth of interpenetration depends on the diffusion coefficient and the time of contact. Sufficient depth of penetration creates a semi-permanent adhesive bone (Figure 2.6).
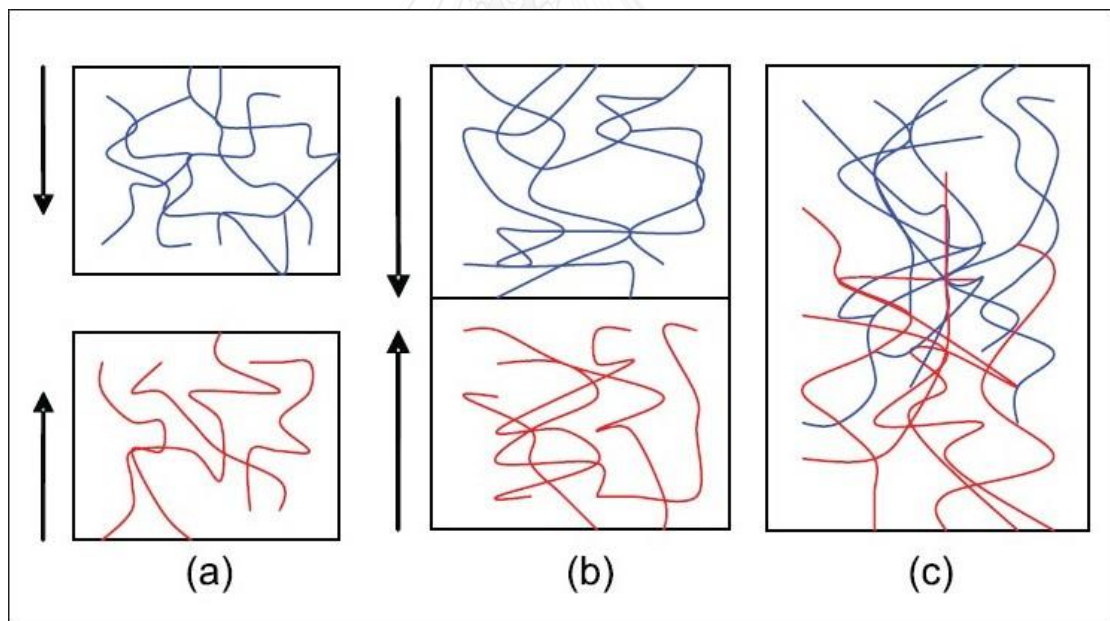
Figure 2.6 (a) Schematic representation of the diffusion theory of bioadhesion. Blue polymer layer and red mucus layer before contact, (b) Upon contact, and (c) The interface becomes diffuse after contact for a period of time [47].

2.2.3.5 Mechanical Theory

Adhesion arises from an interlocking of a liquid adhesive into the micro-cracks and irregularities present on a rough surface. However, rough surfaces also provide an increased surface area available for interaction along with an enhanced viscoelastic and plastic dissipation of energy during joint failure, which are thought to be more important in the adhesion process than a mechanical effect.

2.2.3.6 Fracture Theory

The fracture theory differs a little from the other five in that it relates the adhesive strength to the forces required for the detachment of the two involved surfaces after adhesion. This assumes that the failure of the adhesive bond occurs at the interface. However, failure normally occurs at the weakest component, which is typically a cohesive failure within one of the adhering surfaces.

2.2.4 The mucoadhesive/mucosa interactions

As mentioned above, bioadhesion may take place either by physical or by chemical interactions. For adhesion to occur, molecules must bond across the interface which is interaction forces between mucoadhesive materials and the mucous surface. These bonds can arise in the following way [47].

2.2.4.1 Physical interactions

- Hydrogen bonds

A hydrogen atom, when covalently bonded to electronegative atoms such as oxygen, fluorine or nitrogen, carries a slight positively charge and is therefore is attracted to other electronegative atoms. The hydrogen can therefore be thought of as being shared, and the bond formed is generally weaker than ionic or covalent bonds.

- Van-der-Waals bonds

The Van – der – Waals bonds are some of the weakest forms of interaction that arise from dipole–dipole and dipole-induced dipole attractions in polar molecules, and dispersion forces with non-polar substances.

- Hydrophobic bonds

Hydrophobic bond are more accurately described as the hydrophobic effect, these are indirect bonds (such groups only appear to be attracted to each other) that occur when non-polar groups are present in an aqueous solution. Water molecules adjacent to non-polar groups form hydrogen bonded structures, which lowers the system entropy. There is therefore an increase in the tendency of non-polar groups to associate with each other to minimize this effect.

2.2.4.2 Chemical interactions

- Ionic bonds

The interaction between two oppositely charged ions attract each other via electrostatic interactions to form a strong bond (e.g. in a salt crystal).

- Covalent bonds

Electrons are shared, in pairs, between the bonded atoms in order to "fill" the orbitals in both. These are also strong bonds (e.g. thiomer).

2.2.5 Mucoadhesive polymers

Mucoadhesive polymers may provide an important tool to improve the bioavailability of the active agent by improving the residence time at the delivery site. Mucoadhesive polymers have been also used for coating medical devices. As an example a new generation of intestine inspection device has been recently developed in which mucoadhesive polymer coating make intestinal locomotion possible.

Mucoadhesive polymers have numerous hydrophilic groups, such as hydroxyl, carboxyl, amide, and sulfate to adhere on mucosal tissue. These groups attach to mucus or the cell membrane by various interactions such as hydrogen bonding, hydrophobic, and electrostatic interactions. These hydrophilic groups also cause polymers to swell in water and, thus, expose the maximum number of adhesive sites. An ideal polymer for a bioadhesive drug delivery system should have the following characteristics [48]:

1) The polymer and its degradation products should be nontoxic and nonabsorbable.

2) It should be nonirritant.

3) It should preferably form a strong noncovalent bond with the mucus or epithelial cell surface.

4) It should adhere quickly to moist tissue and possess some site specificity.

5) It should allow easy incorporation of the drug and offer no hindrance to its release.

6) The polymer must not decompose on storage or during the shelf life of the dosage form.

7) The cost of the polymer should not be high so that the prepared dosage form remains competitive.

These materials are natural or synthetic hydrophilic molecules (Table 2.1).

Table 2.1 List of Natural and Synthetic polymers [6, 8, 49-53]

Synthetic polymers	Natural polymers
Cellulose derivatives	Tragacanth
Polycarbophil	Sodium alginate
Poly(acrylic acid)	Karaya gum
Poly(vinyl pyrrolidone)	Guar gum
Poly(vinyl alcohol)	Gelatin
Poly(hydroxyethyl methylacrylate)	Chitosan
Thiolated polymers	Hyaluronic acid

These polymers can be subdivided into three classes: cationic, anionic and nonionic.

- **Cationic polymers** such as chitosan can interact with the mucous surface, since it is negatively charged at physiological pH.

- **Aninonic polymers**, including carboxymethylcellulose and alginates. The alginates, negatively charged polysaccharides, are widely used in the production of microparticles and are frequently reported as polyanionic mucoadhesive polymers. Synthetic polymers derived from poly(acrylic acid)(carbomers) has been considered as a good mucoadhesive material with negatively charged and not water soluble but form viscous gels when hydrated such as polycarbophil.

- **Nonionic polymers**, including hydroxypropylmethylcellulose, hydroxy ethylcellulose and methylcellulose, present weaker mucoadhesion force compared to anionic polymers

The novel mucoadhesive systems such as thiolated polymers are obtained by the addition of conjugated sulfidryl groups increased mucoadhesive properties due to formation of disulfide bridges with cystein domains of glycoproteins of the mucus. An ideal polymer should exhibit the ability to incorporate both hydrophilic and lipophilic drugs. Moreover another study, carried out by Grabovac, Guggi, and

Bernkop-Schnürch (2005) established a ranking of the most studied polymers, showing that both thiolated chitosan and polycarbophil are the most mucoadhesive polymer.

2.2.6 Mucoadhesive polymers dosage form

The primary objectives of mucoadhesive dosage forms are to provide intimate contact of the dosage form with the absorbing surface and to increase the residence time of the dosage form at the absorbing surface to prolong drug action. Mucoadhesive polymers have been utilized in many different dosage forms in efforts to achieve systemic delivery of drugs through the different mucosa in Figure 2.7. These dosage forms include tablets, patches, films, semisolids and powders. To serve as mucoadhesive polymers, the polymers should possess some general physiochemical features such as predominantly anionic hydrophilicity with numerous hydrogen bond-forming groups, suitable surface property for wetting mucus/mucosal tissue surfaces and sufficient flexibility to penetrate the mucus network or tissue crevices. The mucoadhesive drug delivery system may include the following [54].

1. Gastrointestinal delivery system.

2. Nasal delivery system.

3. Ocular delivery system.

4. Buccal delivery system.

5. Vaginal delivery system.

6. Rectal delivery system.
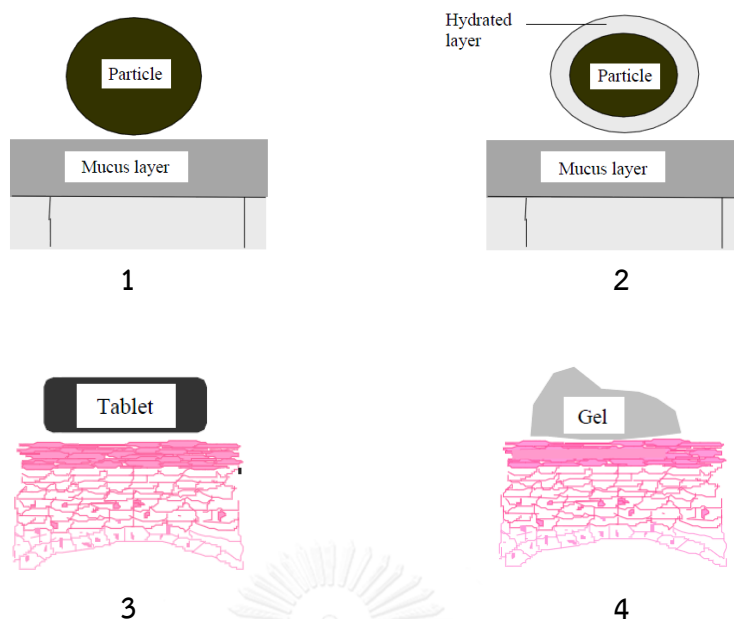
Figure 2.7 Some scenarios where mucoadhesion can occur [47].

1. Dry or partially hydrated dosage forms contacting surfaces with substantial mucus layers (e.g. aerosolised particles deposited in the nasal cavity).

2. Fully hydrated dosage forms contacting surfaces with substantial mucus layers (e.g. particle suspensions in the gastrointestinal tract).

3. Dry or partially hydrated dosage forms contacting surfaces with thin/ discontinuous mucus layers (e.g. a tablet placed onto the oral mucosa).

4. Fully hydrated dosage forms contacting surfaces with thin/discontinuous mucus layers (e.g. aqueous microparticles administered into the vagina).

2.3 Chitosan

Chitosan was discovered by Rouget in 1859 after boiling chitin in concentrated potassium hydroxide and was given a formally name by Hoppe-Seyler in 1894. It was a form of fiber chemically biopolysaccharide processed from outer skeletons of arthropods, the epidermis of crustacean shells such as shrimp and crabs shells, prawns, lobsters, and cell walls of some fungi such as *aspergillus* and *mucor*.

2.3.1 Structure of chitosan

Chitosan $(C_6H_{11}O_4N)_n$ is a linear polycationic biopolyaminosaccharide with high molecular weight composed of randomly distributed β-(1-4)-linked 2-acetamido-2-deoxy-*D*-glucopyranose and 2-amino-2-deoxy-*D*-glucopyranose (Figure 2.8). It was obtained on commercially industrial scales by thermo-alkaline *N*-deacetylation of chitin which can be controlled by time, temperature, and concentration of alkaline treatment [55]. Therefore, the degree of deacetylation has significant effect on the solubility, rheological properties, and biological properties of chitosan [56]. NMR spectroscopy was used to determine deacetylation of chitosan and showed in the range of 60-100% for commercial scale. The chemical structure of a fraction of the repeating units of chitosan backbone contains hydroxyl groups (-OH) and amine pendent groups (-NH$_2$) while the rest contains acetamide group (-NHCO) in its place. Both hydroxyl groups and reactive primary amine groups can be used to chemically alter its properties under mild reaction conditions [57].
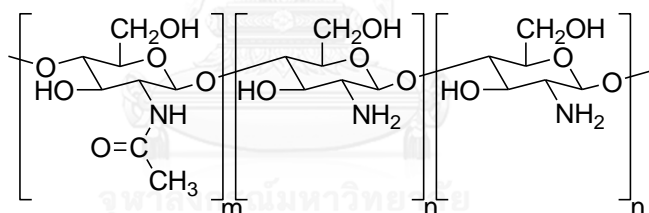
Figure 2.8 Chemical structure of chitosan

2.3.2 Physico-chemical properties of chitosan

Chitosan is firmly established as a biodegradable, biocompatible, low toxic, and mucoadhesive polymer [58]. It is a cationic polysaccharide that can be degraded by several enzymes such as chitinases which are secreted by intestinal microorganisms, lysozyme which is highly concentrated in mucosal surfaces and by human chitotriosidase [59]. Chitosan exhibits the capacity to promote the absorption of poorly absorbed macromolecules across epithelial barriers by transient widening of cell tight junctions casing high mucoadhesive properties for drug delivery system [60]. Moreover, it is also a known antimicrobial agent against various bacteria such as

Escherichia coil [61-63]. Chitosan is a weak base with pK_a of the *D*-glucosamine residue about 6.2-7.0, therefore; it is insoluble at neutral and alkaline pH values. However, chitosan provided salt with inorganic and organic acids by dissolving in acetic acid, hydrochloric acid, glutamic acid, and lactic acid to improve the solubility. The solubility of chitosan depends on degree of deacetylation and pH of solution providing the protonated positive charge of amino group.

2.3.3 Pharmaceutical applications

Recently, chitosan has been a variety of promising pharmaceutical uses and is presently considered as a novel carrier material in drug delivery systems [64]. Chitosan was evaluated in the form of beads [65], microsphere [66], microcapsules [67], tablets [68], and also used as a matrix for sustained release [69], a component of gels [70], and membranes [71].

Due to its low-toxicity, biocompatibility with human body tissue, chitosan has displayed their effectiveness for all forms of dressings-artificial skin, corneal bandages, and suture thread in surgery-as well as for implants in bone repair or dental surgery [72]. Lastly, chitosan is an excellent medium for carrying and slow release of medicinal active principles in plants, animals, and man. If degree of deacetylation and molecular weight can be controlled, it would be good advantage for developing size of chitosan for drug delivery system [73].

2.3.4 Mucoadhesive chitosan

Chitosan exhibited strong mucosal adhesion based on electronic interactions of cationic chitosan with negatively charged mucin [74]. Interactions with mucin appear to be both electrostatic, via NH_3^+ groups on the chitosan with either COO^- or SO_3^- groups on the mucin carbohydrate side chains and/or hydrophobic, via $-CH_3$ groups on acetylated chitosan residues with $-CH_3$ groups on mucin side chains (depending on the degree of acetylation of the chitosan, local solvent conditions, for example, pH, ionic strength, and the degree of sulphonation and sialic acid content of the mucin). Moreover, these dramatic changes in solution turbidity are related to

the aggregation of mucin particles in the presence of small portions of chitosan and subsequent disaggregation caused by excess of the cationic polymer in the solution (Figure 2.9).
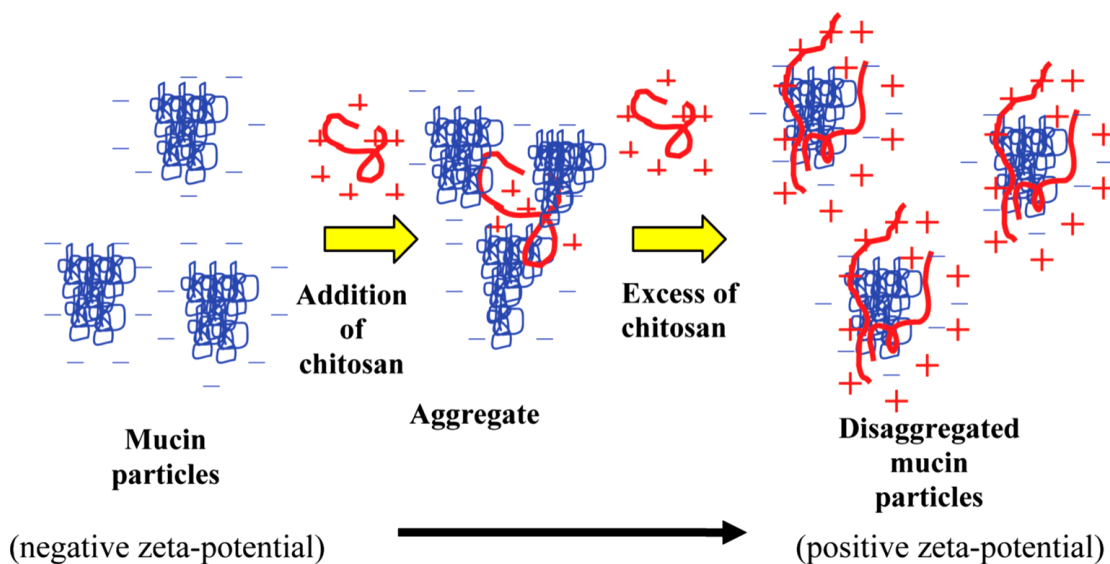
Figure 2.9 Diagram depicting aggregation/disaggregation of pig gastric mucin in the presence of mucin [18].

2.4 Carbodiimide

A Carbodiimide or methanediimine is a carboxyl-reactive chemical group consisting of the formula RN=C=NR. It hydrolyzes to form ureas or thioureas making them rarely found in nature. Carbodiimide provides the most popular and versatile method and was often used to activate carboxylic acids in order to produce the amide or ester functional group such as occur in proteins crosslinking, peptide synthesis to nucleic acid, preparation of immunoconjugates and many other biomolecules. Additives, such as *N*-hydroxybenzotriazole or *N*-hydroxysuccinimide, are often added to increase yields and decrease side reactions.

The water soluble 1-ethyl-3-(3-dimethylaminopropyl) carbodiimide hydrochloride (EDAC) and the water insoluble *N',N'*-dicryclohexyl carbodiimide (DDC) were the most readily available and commonly used carbodiimides for using as aqueous and non-aqueous organic synthesis, respectively (Figure 2.10).

Figure 2.10 Chemical structures of EDAC and DCC.

2.4.1 Reaction of EDAC carbodiimide crosslinker

EDAC (also EDC or EDCI) is a water soluble carbodiimide which is typically efficient in acidic (pH 4.5) condition. It is generally used to react with carboxylic groups to form an active *O*-acylisourea intermediate which is easily displaced by nucleophilic attack from primary amino groups in the reaction mixture (Figure 2.11). The formation of an amide bone using EDAC is straightforward, but with several side effects complicating the subject. The primary amine forms an amide bond with the original carboxyl group and a soluble isourea derivative as EDAC by product is released. Because the *O*-acylisourea intermediate is unstable in aqueous solution, it fails to react with an amine resulting in hydrolysis of the intermediate. The use of solvents with low-dielectric constants such as dichloromethane or chloroform can minimize this side reaction.
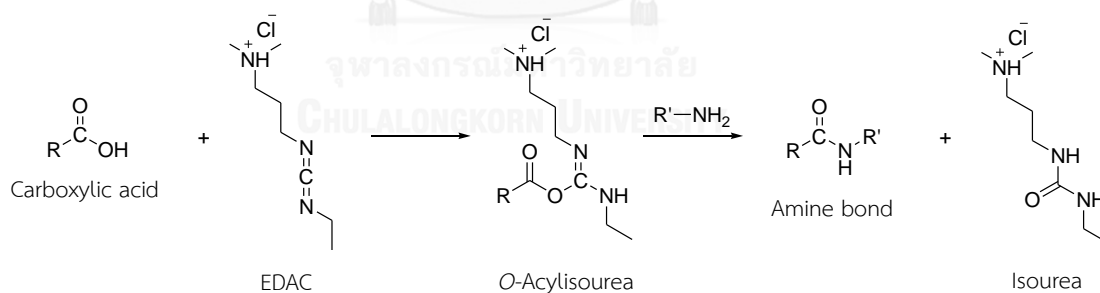
Figure 2.11 Carboxyl-to-amine crosslinking with the popular carbodiimide, EDAC.

Additionally, EDAC is often used in combination with *N*-hydroxysuccinimide (NHS) or its water soluble sulfo-NHS to increase coupling efficiency or create a stable amine reactive intermediate (Figure 2.12). EDAC couples NHS to carboxyls, forming an NHS eater that is considerably more stable than the *O*-acylisourea intermediate while allowing for efficient conjugation to primary amines at physiologic pH. EDAC can also be used to activate phosphate groups in the presence of imidazole for conjugation

to primary amine. The method is sometimes used to modify, label, crosslink or immobilize oligonucleotides through their 5' phosphate groups.
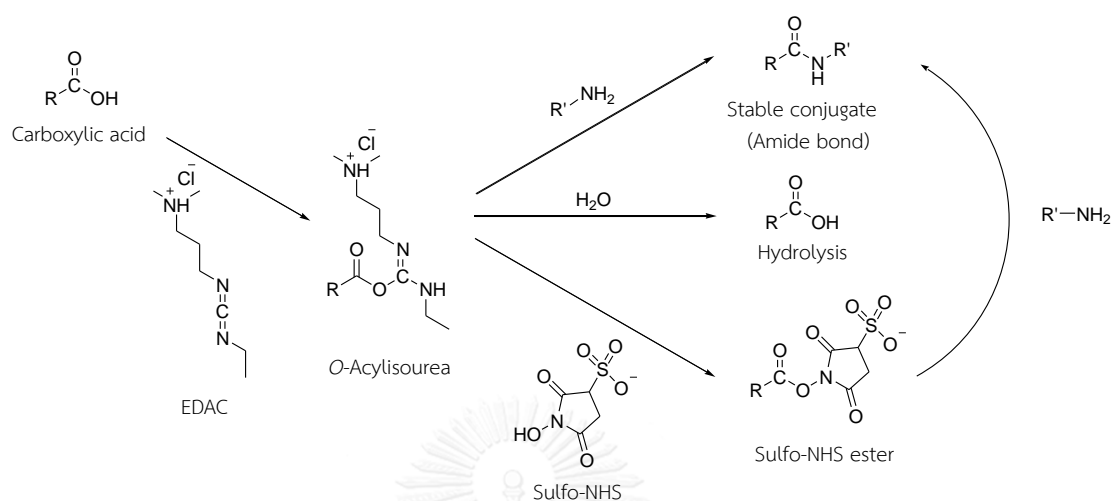
Figure 2.12 Carboxyl-to-amine crosslinking using the carbodiimide, EDAC and sulfo-NHS.

2.4.2 Application of EDAC crosslinking

EDAC is a powerful and versatile tool for crosslinking of primary amines to carboxylic acid groups. Peptides and proteins contain both primary amines and carboxylic acid (N- and C-termini, respectively, as well as in the side-chain of certain amino acids). Therefore, EDAC enables peptides and proteins to be easily conjugated to one another or to any compounds or solid surfaces that bear either carboxyl or amino groups and can use in the applications as follows.

-Peptide conjugation to carrier proteins

-Label carboxyl groups with amine compounds

-Immobilize peptides for affinity purification

-Attach peptides to surface materials

CHAPTER III

EXPERIMENTAL

3.1 Materials

3.1.1 Polymer

Chitosan, food grade, M_w 500 kDa., Deacetylation 85 %, Lot No. 497613, (Seafresh Chitosan (Lab.) Co., Ltd. in Thailand)

3.1.2 Chemicals

- Acetic acid (AcOH), AR grade (Union chemicals)

- Acetone, commercial grade (Merck, Germany)

- Basic fuchsin (pararosaniline), analytical grade (Sigma-Aldrich, USA)

- *N*-(3-chloro-2-hydroxy-propyl)trimethylammonium chloride (Quat-188), analytical grade (TCl Co., Ltd.)

- 4-Carboxybenzenesulfonamide (4-CBS) 97 %, AR grade (Sigma-Aldrich, USA)

- Deuterium oxide (D$_2$O), NMR spectroscopy grade (Merck, Germany)

- Ethanol (EtOH) 95 %, commercial grade (Merck, Germany)

- 1-Ethyl-3-(3-dimethylaminopropyl)carbodiimide hydrochloride (EDAC), analytical grade (Sigma-Aldrich, USA)

- Hydrochloric acid (HCl) fuming 37 %, AR grade (Merck, Germany)

- *N*-hydroxysuccinimide (NHS), AR grade (Sigma-Aldrich, USA)

- Iodine, AR grade (Sigma-Aldrich, USA)

- Methanol (MeOH), commercial grade (Merck, Germany)

- Methyl iodide (CH$_3$I), AR grade (Sigma-Aldrich, USA)

- Mucin from porcine stomach (type 2), analytical grade (Sigma-Aldrich, USA)

- *N*-methyl pyrolidone (NMP), AR grade (Merck, Germany)

- Oleoyl chloride, analytical grade (TCl Co., Ltd.)

- Periodic acid, analytical grade (Sigma-Aldrich, USA)

- Potassium bromide (KBr), AR grade (Merck, Germany)

- Potassium dihydrogen phosphate (KH_2PO_4), AR grade (Merck, Germany)

- Potassium chloride (KCl), AR grade (Merck, Germany)

- Sodium bicarbonate (Na_2CO_3), AR grade (Merck, Germany)

- Sodium chloride (NaCl), AR grade (Merck, Germany)

- Sodium hydrogen phosphate (Na_2HPO_4), AR grade (Merck, Germany)

- Sodium hydroxide (NaOH), AR grade (Merck, Germany)

- Sodium metabisulfite ($Na_2S_2O_5$), analytical grade (Sigma-Aldrich, USA)

- Trifluoroacetic acid (CF_3COOH), analytical grade (Sigma-Aldrich, USA)

3.1.3 Dialysis membrane

Dialysis membrane with molecular weight cut-off (MWCO) at 12,000-14,000 Da (Membrane Filtration Product, Inc.) is used to purify all modified chitosan.

3.2 Instruments

The instruments used in this study are listed in Table 3.1

Table 3.1 The instruments in this study

Instrument	Manufacture	Model
FT-IR spectrometer	Nicolet	6700
Incubator	IKA	KS 4000 i
Micropipette	Mettler Toledo	Volumate
^{1}H NMR spectrometer	Varian	400 MHz
pH meter	Metrohm	744
Scanning Electron Microscope	Philips	XL30CP
Small bench centrifuge	Hettich	EBA20
UV-VIS spectrometer	Perkin Elmer	Lumbda 80
Vortex	Scientific industries	Vortex-genie-V2

3.3 Methods

3.3.1 Synthesis of OA-4-CBS-QCS

3.3.1.1 Synthesis of quaternized chitosan (QCS)

3.3.1.1.1 Synthesis of *N*-trimethyl chitosan chloride (TMC)

TMC was synthesized according to previously reported procedures [75, 76]. Briefly, the mixture of (100 mL) of a 1% (w/v) of chitosan in 1% (v/v) acetic acid solution, (5 mL) of 15% (w/v) aqueous sodium hydroxide and (15, 30 mL) of methyl iodide (CH$_3$I) in (15, 30 mL) of *N*-methyl pyrolidone (NMP) were heated at a temperature 60 C° for 45 min. The product was precipitated with (1 L) of 80 % (v/v) ethanol in acetone. Therefore, the precipitate was filtered, dissolved in (40 mL) of (5% w/v) aqueous sodium chloride solution to exchange the iodide ion with a chloride ion. The suspension was dialyzed with distilled water (3 × 1 L) to remove inorganic materials. The dialyzed solution was precipitated with acetone and then

recovered by filtration. The precipitate was obtained then collected and dried overnight at room temperature.

3.3.1.1.2 Synthesis of chitosan *N*-(3-chloro-2-hydroxy-propyl) trimethylammonium chloride (CS Quat-188)

Preparation of regenerated chitosan

Chitosan (0.50 g) was dissolved in (100 mL) of 1% (v/v) acetic acid solution. This solution was stirred at room temperature overnight and dropped slowly into 2% (w/v) aqueous sodium bicarbonate, in an distilled water/methanol mixture (distilled water/methanol = 40/60 (v/v)), (100 mL). The pH of the solution was adjusted to pH 9 by the addition 15% (w/v) aqueous sodium hydroxide. The regenerated chitosan was then recovered by filtration and kept while still moist before the next synthesis step [24].

Quaternization of *N*-substituted chitosan using Quat-188 (CS Quat-188)

(1, 15, 20 mL) of 65% (w/w) aqueous solution of Quat-188 was added to the reaction flask and the pH of the solution was raised to pH 8 by using 15% (w/v) sodium hydroxide. Then iodine (0.25 g) was added along with the regenerated chitosan while still moist. The solution was stirred for 48 h at room temperature, (50 mL) of distilled water was added, and the temperature was raised to 50 °C for stirring another 24 h. After quaternization, quaternized chitosan was dissolved in 15% (w/v) aqueous sodium chloride solution in order to replace the iodide ion by chloride ion. The suspension was dialyzed with distilled water (3 × 1 L) to remove inorganic materials. The dialyzed solution was then concentrated under vacuum using a rotary evaporator. The concentrated solution obtained was then collected and dried overnight at room temperature [24].

3.3.1.2 Synthesis of 4-carboxybenzenesulfonamide-Quaternized chitosan (4-CBS-QCS) conjugates

Quaternized chitosan was fully dissolved (0.01 g/mL) in 1% (v/v) acetic acid solution at room temperature overnight to perform (100 ml) of quaternized chitosan solution, and then 4-CBS (0.2 g), EDAC (0.25 g), and NHS (0.15 g) were added to the mixture as schematically summarized in Figure 3.1. The reaction mixture was refluxed at 60 °C for 24 h to form the 4-CBS-QCS. The mixture was precipitated with 1 N aqueous sodium hydroxide and dialyzed in ethanol (3 × 1 L) to removed excess EDAC, NHS, NaOH, and unreacted 4-CBS. Finally, the dialyzed solution was then concentrated under vacuum using a rotary evaporator. The concentrated solution was obtained then collected and dried overnight at room temperature [25].

3.3.1.3 Synthesis of oleoyl-4-carboxybenzenesulfonamide-quaternized chitosan (OA-4-CBS-QCS) conjugates

4-CBS-QCS was fully dissolved (0.01 g/mL) in 1% (v/v) acetic acid solution at room temperature overnight to perform (20 ml) of 4-CBS-QCS solution. Oleoyl chloride (0.11 ml), EDAC (0.25 g), and NHS (0.15 g) were dissolved in (7 ml) of an ethanol/acetone mixture (ethanol/acetone = 2/5 (v/v)) and then heated at 60 °C for 1 h. The solution was added into the 4-CBS-QCS solution, followed by stirred and refluxed at 60 °C for another 24 h as schematically summarized in Figure 3.1. The suspension was dialyzed with distilled water (3 × 1 L) using a dialysis membrane to remove excess EDAC, NHS, and unreacted OA and dried under vacuum. Finally, the dialyzed solution was then concentrated under vacuum using a rotary evaporator. The concentrated solution was obtained then collected and dried overnight at room temperature.
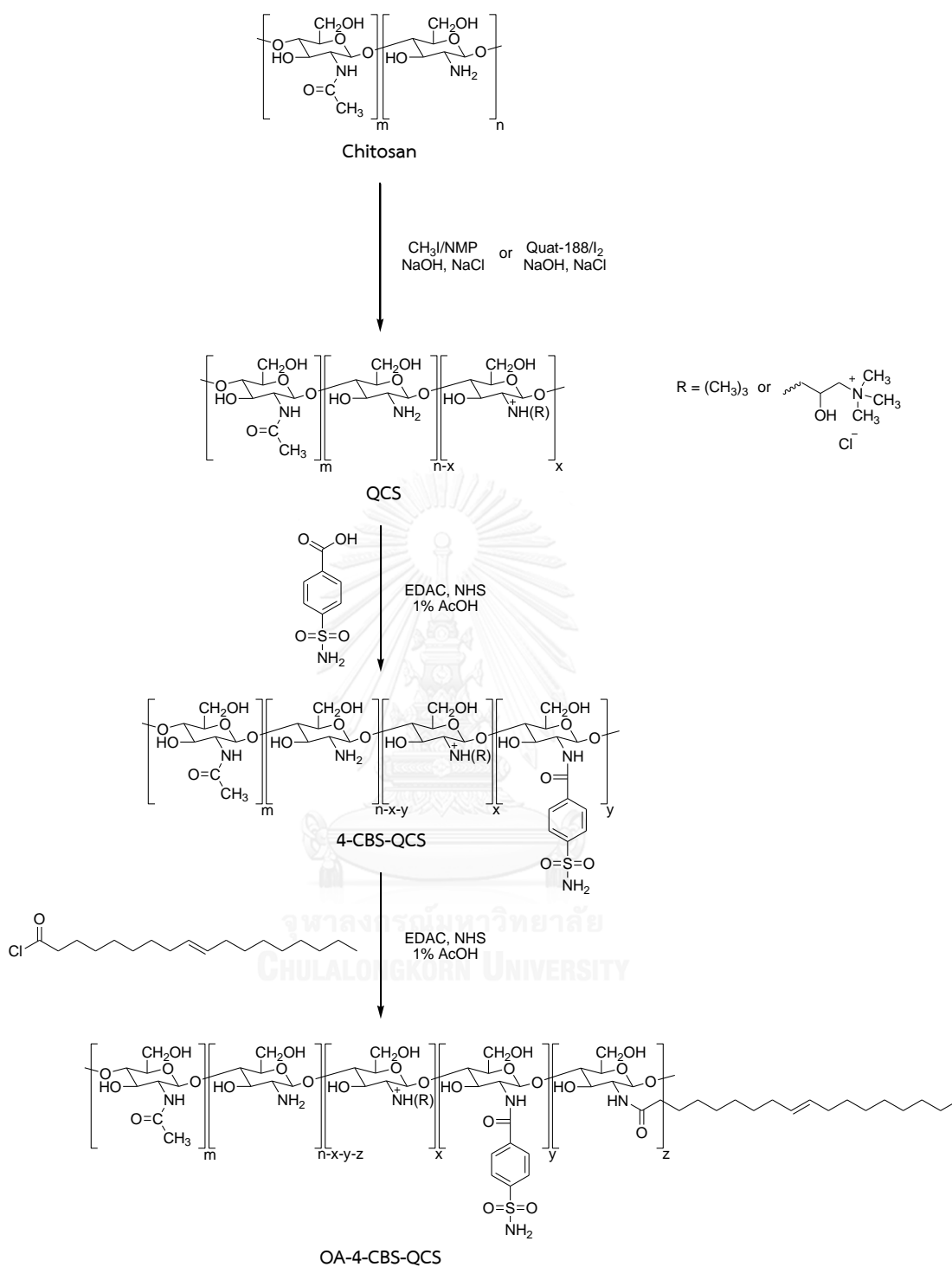
Figure 3.1 Synthesis scheme of oleoyl-4-carboxybenzenesulfonamide-quaternized chitosan (OA-4-CBS-QCS)

3.3.2 Chemical characterizations

3.3.2.1 Fourier transformed infrared spectroscopy (FT-IR)

The chitosan, QCS, 4-CBS-QCS, and OA-4-CBS-QCS were dried and ground into a fine powder. The powder then was mixed with potassium bromide (KBr) at 1:100 (w/w) to the powder in agate mortar and pestle. The mixture was then transferred to a hydraulic pressing machine and pressed into a pellet. Analysis was performed by a Nicolet 6700 Fourier transformed infrared (FT-IR) spectrometer system, scanning from 600 to 4000 cm^{-1}.

3.3.2.2 ^{1}H Nuclear Magnetic Resonance spectroscopy (^{1}H NMR)

For the characterization of chitosan, QCS, 4-CBS-QCS, and OA-4-CBS-QCS, 5 mg of each compound were dissolved in 2% (v/v) trifluoroacetic acid (CF_3COOH) in deuterium oxide (D_2O). ^{1}H NMR spectra were recorded by a Mercury Varian NMR spectrometer operated at 400 MHz (Agilent Technologies, CA, USA), using pulse accumulating of 64 scans.

3.3.2.3 Determination of the degree of quaternization (%DQ) and the degree of substitution (%DS)

The degree of quaternization of the quaternized chitosan and the degree of substitution of chitin, chitosan, 4-CBS and OA were determined by ^{1}H NMR spectra using 2% (v/v) trifluoroacetic acid (CF_3COOH) in deuterium oxide (D_2O) and calculated using equation (1), (2), (3), (4) and (5), respectively [77, 78].

$$\%DS_{chitin} = \left[\frac{I_{(NHCOCH_3)}}{I_{(H_3-H_6)}} \times \frac{5}{3} \right] \times 100 \quad \ldots\ldots(1)$$

Where, $I_{(NHCOCH_3)}$ is the integral area of GlcNAc protons and $I_{(H_3-H_6)}$ is the integral area of protons at the C3 - C6 carbon of the GluN units.

$$\%DS_{chitosan} = 100 - \%DS_{chitin} \quad \ldots\ldots(2)$$

$$\%DQ_{QCS} = \left[\frac{I_{(CH_3)_3}}{I_{(H_3-H_6)}} \times \frac{5}{9} \right] \times 100 \quad ......(3)$$

Where, $I_{(CH_3)_3}$ is the integral area of quaternized amino group protons and $I_{(H_3-H_6)}$ is the integral area of protons at the C3 - C6 carbon of the GluN units.

$$\%DS_{4\text{-CBS-QCS}} = \left[\frac{I_{(SO_2NH_2)}}{I_{(H_3-H_6)}} \times \frac{5}{4} \right] \times 100 \quad ......(4)$$

Where, $I_{(SO_2NH_2)}$ is the integral area of the benzene ring of 4-CBS-QCS protons and $I_{(H_3-H_6)}$ is the integral area of protons at the C3 - C6 carbon of the GluN units.

$$\%DS_{OA\text{-4-CBS-QCS}} = \left[\frac{I_{(a)}}{I_{(H_3-H_6)}} \times \frac{5}{3} \right] \times 100 \quad ......(5)$$

Where, $I_{(a)}$ is the integral area of methyl of OA-4-CBS-QCS protons and $I_{(H_3-H_6)}$ is the integral area of protons at the C3 - C6 carbon of the GluN units.

3.3.3 *In vitro* bioadhesion of mucin to chitosan and the modified chitosan

3.3.3.1 Mucin glycoprotein assay

The Periodic Acid Schiff (PAS) colorimetric method is widely used for both quantitative and qualitative analysis of mucins, glycoproteins, glycogen and other polysaccharides in tissues and cells [79]. The PAS colorimetric assay used for the detection of glycoproteins was used to determine the free mucin concentration, so as to evaluate the amount of mucin adsorbed onto the chitosan, QCS, 4-CBS-QCS, and OA-4-CBS-QCS. Two reagents were prepared. Schiff reagent contained 1% (w/v) basic fuchsin (pararosaniline) was dissolved in DI water. 20 mL of 1 M HCl and 0.1 g of sodium metabisulphite was added to every 6 mL of fuchsin solution. The resultant

solution was incubated at 37°C until it became colorless or pale yellow. The solution was filtered before use. The PAS reagent was freshly prepared by adding 10 μL of 50% (v/v) periodic acid solution to 7 mL of 7% (v/v) acetic acid solution.

3.3.3.2 Adsorption of mucin on chitosan and modified chitosan

0.5% (w/v) mucin solution in two different of pH, namely the simulated gastric fluid (SGF, pH 1.2) and simulated intestinal fluid (SIF, pH 6.4) media were prepared chitosan, QCS, 4-CBS-QCS, and OA-4-CBS-QCS were dispersed (at 1 mg/mL final) in the above mucin solutions. These were mixed, vortexed and shaken at 37 °C for 3 h. Then the dispersions were centrifuged at 12,000 rpm for 2 min to pellet the polymer-mucin and the supernatant was harvested and used for the measurement of the free mucin content. The mucin concentration was calculated by reference to the calibration curve, and the amount of mucin adsorbed to the polymers was calculated as the difference between the total amount of mucin added and the free mucin content in the supernatant. Standard calibration curves were prepared from the five mucin standard solutions (0.1, 0.2, 0.3, 0.4, and 0.5 mg/mL). After adding 100 μL of dilute periodic acid reagent, the solution were incubated at 37 °C for 2 h. Then, 100 μL of Schiff reagent was added at room temperature for 30 min. Next, 100 μL aliquots of the solution were transferred in triplicate into a 96-well microtiter plate and the absorbance at 555 nm was recorded. The mucin contents were then calculated by reference to the standard calibration curve.

3.3.4 Scanning Electron Microscopy (SEM)

The morphology and surface appearance of the OA-4-CBS-QCS with different re-dispersed concentration were examined by SEM (Philips, XL30CP). The self-assembly of OA-4-CBS-QCS particles were prepared by re-dispersed in distilled water with a concentration of 0.3, 1.3, 2.3, 3.3, and 4.3 mg/mL and then shaken by high vortex for 2 h at room temperature. Each sample solution was dropped on the clean surface of the glass slide and dried in desiccator for 2 days. The glass slide of

each sample were adhered to the aluminum stub using double-sided carbon adhesive tape and coated with gold-palladium. Coating was achieved at 50 mA for 6 min through a sputter coater. The particles were observed via scanning electron microscope under high vacuum at an ambient temperature with a beam voltage of 15 kV.

CHAPTER IV

RESULTS AND DISCUSSION

4.1 Synthesis and structural analysis of OA-4-CBS-QCS

Quaternization of chitosan was carried out using methyl iodide (CH_3I) or *N*-(3-chloro-2-hydroxy-propyl)trimethylammonium chloride (Quat-188) as the quaternizing agent which reacted with either the primary amino groups of the glucosamine residue of chitosan in a nucleophilic substitution pathway to introduce the quaternary ammonium substituent.

The carboxylic acid groups (-COOH) of 4-CBS and OA were activated by EDAC as a coupling reaction to form an *O*-acylisourea ester as the unstable intermediate product. Therefore, NHS was added to improve the efficiency of EDAC coupling reactions by forming NHS-ester that is stable enough to reacts with the primary amine groups (-NH_2) of quaternized chitosan to form 4-CBS-QCS and OA-4-CBS-QCS as a result conjugated via amide bond, as shown schematically in Figure 4.1. The resulting OA-4-CBS-QCS appeared as a white and odorless powder. They were easily dissolved in distilled water to form nanofractal hyperbranch polymer. The obtained OA-4-CBS-QCS were characterized by FT-IR and ^{1}H NMR analysis.
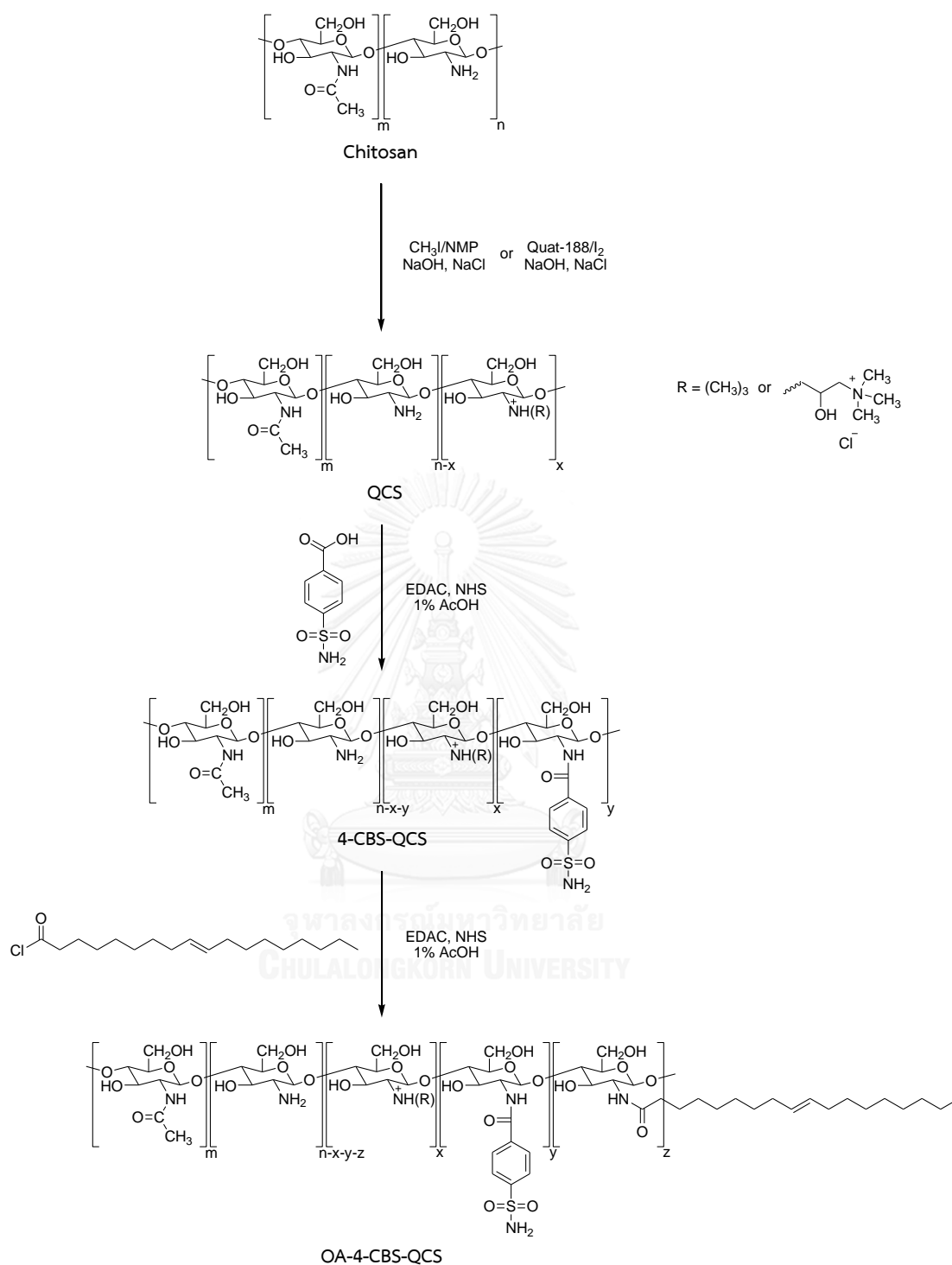
Figure 4.1 Synthesis scheme of oleoyl-4-carboxybenzenesulfonamide-quaternized chitosan (OA-4-CBS-QCS)

4.2 Characterization and physical properties of chitosan, QCS, 4-CBS-QCS, and OA-4-CBS-QCS.

4.2.1 Fourier transformed infrared spectroscopy (FT-IR)

The FT-IR spectra of chitosan, QCS, 4-CBS-QCS, and OA-4-CBS-QCS are showed in Figures 4.2 and 4.3. The FT-IR spectrum of chitosan (Figure 4.2a) showed a broad absorption peak at 3418 cm^{-1} corresponding to O-H and N-H symmetrical stretching vibrations and the typical bands of symmetric C-H stretching vibrations showed at 2923 cm^{-1} and 2878 cm^{-1} attributed to pyranose ring [80], Peaks at 1637, 1420, 1377, 1077 cm^{-1} were assigned to C=O stretching of amide I, -CH_2 bending, -CH_3 symmetrical deformation and skeletal vibration of C-O stretching, respectively. After quaternization of the CH_3I and Quat-188 onto the C2-amine groups of chitosan, the FT-IR patterns showed the characteristic peaks at 1562 cm^{-1} (TMC) (Figure 4.2b) and 1557 cm^{-1} (CS Quat-188) (Figure 4.2c) attributed to N-H bending of amide II. New peaks at 1458 cm^{-1} (TMC) and 1480 cm^{-1} (CS Quat-188) were due to C-H symmetric bending of methyl substituent of the quaternary ammonium groups [81-83]. Moreover, the broad overlapping bands and the decreasing of intensity in the 1158 to 852 cm^{-1} range that result from the coupling of the C-N axial stretching and N-H angular deformation range.

In addition, the 4-CBS-TMC (Figure 4.3d) and 4-CBS-CS Quat-188 spectra (Figure 4.3e) revealed the characteristic peaks of both 4-CBS and TMC, CS Quat-188. Increase of the width peak at 3419 cm^{-1} (4-CBS-TMC) and 3413 cm^{-1} (4-CBS-CS Quat-188) due to the N-H stretching overlapped to the O-H stretching and overlapped to the C-H aromatic ring. The peak at 1646 cm^{-1} (4-CBS-TMC) and 1646 cm^{-1} (4-CBS-CS Quat-188) assigned to C=O stretching of amide II, C=C aromatic ring stretching of 4-CBS and overlapped with the amide I and amide II band stretching of chitosan.

Finally, the FT-IR spectra of the OA-4-CBS-TMC (Figure 4.3f) and OA-4-CBS-CS Quat-188 (Figure 4.3g) showed similar the characteristic peaks of 4-CBS-TMC and 4-CBS-CS Quat-188. Increase of the intensity peak at 2855-2925 cm^{-1} (OA-4-CBS-TMC)

and 2853-2922 cm^{-1} (OA-4-CBS-CS Quat-188)   range assigned to C-H aliphatic stretching of long chain hydrocarbons of OA substituent and the peak at 1650 cm^{-1} (OA-4-CBS-TMC) and 1635 cm^{-1} (OA-4-CBS-CS Quat-188) were assigned to C=O stretching of amide II, C=C aromatic ring stretching of 4-CBS, C=O stretching of OA and overlapped with the amide I and amide II band stretching of chitosan. These results support that the OA-4-CBS-TMC and OA-4-CBS- CS Quat-188 were successfully prepared.
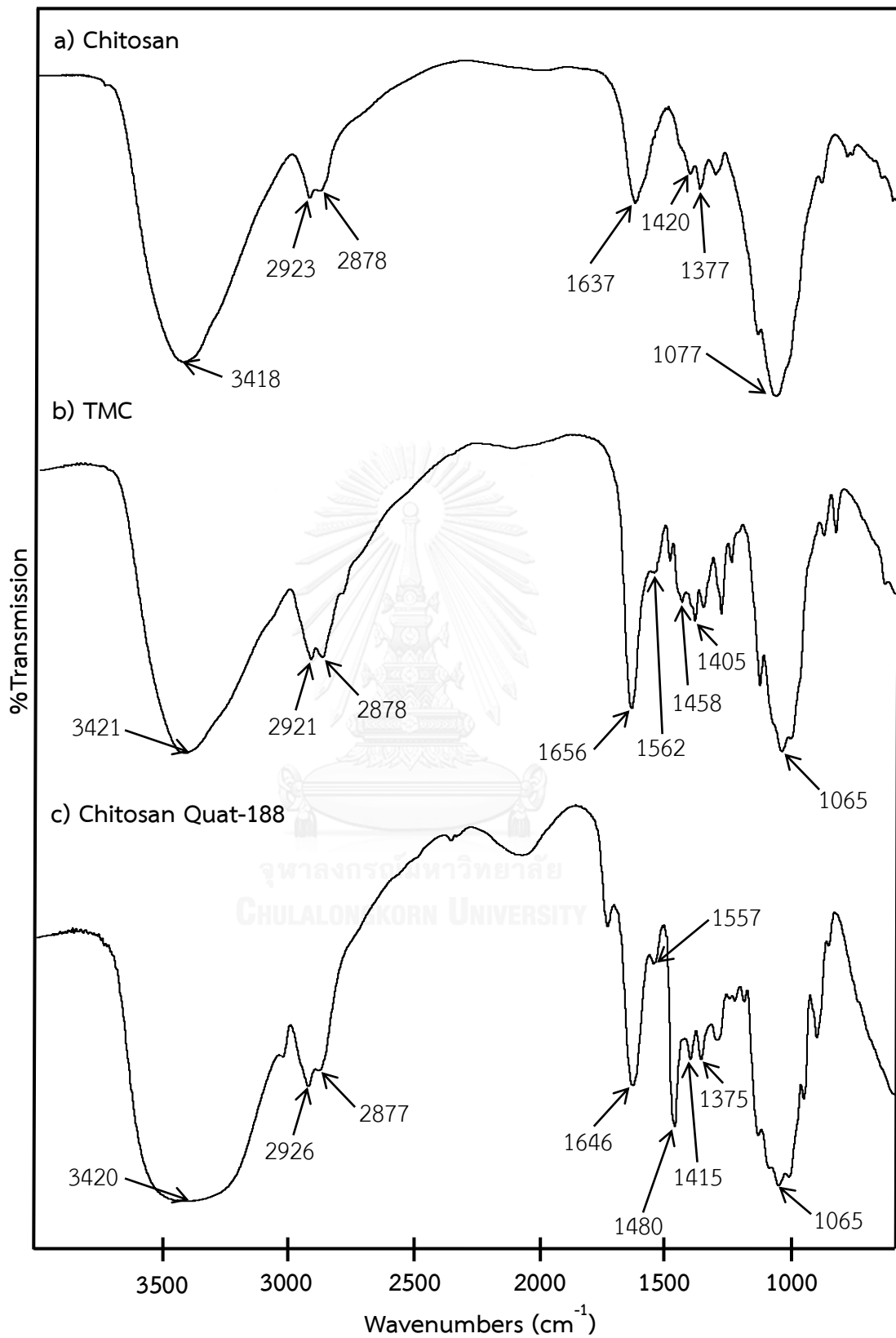
Figure 4.2 FT-IR spectra of the a) CS, b) TMC, and c) CS Quat-188
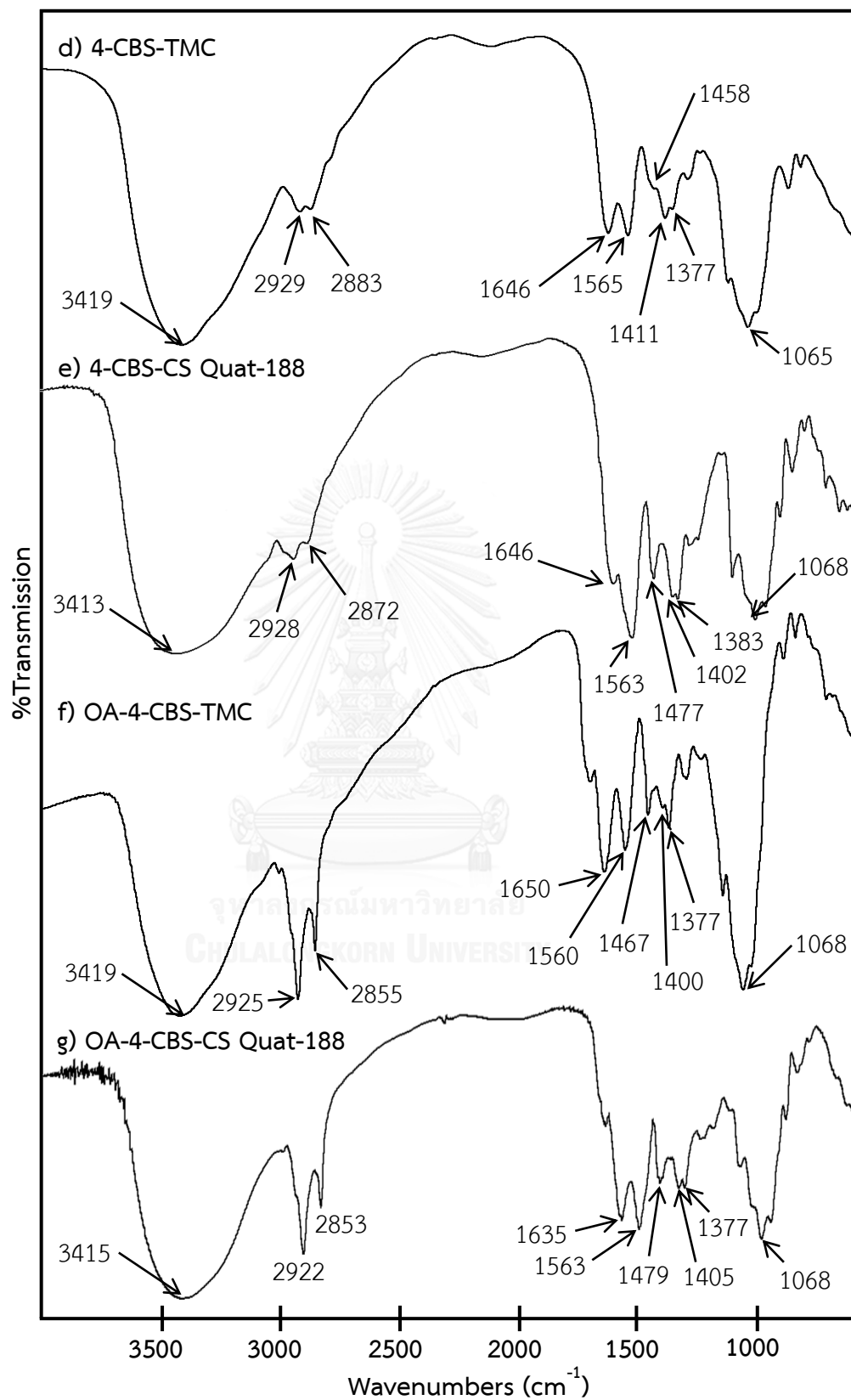
Figure 4.3 FT-IR spectra of the d) 4-CBS-TMC, e) 4-CBS-CS Quat-188, f) OA-4-CBS-TMC, and g) OA-4-CBS-CS Quat-188

4.2.2 [1]H Nuclear Magnetic Resonance spectroscopy (^{1}H NMR)

The chemical structures of chitosan, QCS, 4-CBS-QCS and OA-4-CBS-QCS were characterized by ^{1}H NMR spectroscopy as showed in Figures 4.4, 4.5 and 4.6. The ^{1}H NMR spectrum of chitosan (Figure 4.4a) showed peak at 2.08 ppm (s, 3H) for the acetyl protons of the GluNAc units, 3.19 ppm (s, 1H) attributed to the H at the carbon 2 of the GluN units, whilst the peaks due to the H at the carbon 3 to 6 in the GluNAc and GluN units were observed at around 3.73-3.92 ppm (m, 5H) and peak at 4.77 ppm for the H at the carbon 1.

The ^{1}H NMR spectra of TMC (Figures 4.4b and 4.4c) showed new peak at 2.76 ppm (m, 6H) for dimethyl amino group ($N(CH_3)_2$) and peak at 2.99 ppm (m, 9H) for quaternized amino group ($N^+(CH_3)_3$), as well as at 3.25 ppm (s, 3H) for O-methylated group (OCH_3). Apart from these, the peak at 2.01 ppm (s, 3H), 3.42 ppm (s, 1H), 3.46-4.16 ppm (m, 5H) and 5.36 ppm (s, 1H) were assigned to the acetyl protons of the GluNAc units, H at the carbon 2, H at the carbons 3 to 6 and H at the carbon 1 in the GluNAc, respectively. Cause a shifting to higher chemical shift and higher intensity of signal hydrogen atom bonded to the carbon atoms 1 to 6 of the GluNAc and GluN units due to steric effect of quaternized and dimethyl amino group.

The ^{1}H NMR spectra of CS Quat-188 (Figures 4.5d, 4.5e and 4.5f) showed new peaks at 2.87 ppm for methylene protons ($C\underline{H}_2NH$, a), 3.33 ppm for quaternized amino group (($C\underline{H}_3)_3N^+$,d), as well as 3.52 ppm for methylene protons ($C\underline{H}_2N^+(CH_3)_3$, c) and 4.42 ppm for methane protons ($C\underline{H}OH$, b). Apart from these, the peaks at 2.16 ppm (s, 3H), 3.02 ppm (s, 1H), 3.50-4.65 ppm (m, 5H) and 4.52 ppm (s, 1H) were assigned to the acetyl protons of the GluNAc units, H at the carbon 2, H at the carbons 3 to 6 and H at the carbon 1 in the GluNAc, respectively. Cause a shifting to higher chemical shift and higher intensity of signal hydrogen atom bonded to the carbon atoms 1 to 6 and 6' of the GluNAc and GluN units due to steric effect of quaternized amino group.

The ^{1}H NMR spectrum of 4-CBS-TMC (Figure 4.6g) showed the characteristic peaks of both TMC and 4-CBS segments. The aromatic proton position of the

sulfonamide ring showed at 7.96 ppm (d, 2H) and 7.77 ppm (d, 2H). Both the GluNAc and GluN units contributed to the peak at 5.03 ppm for H at the carbon 1 and peak at 4.16-3.75 ppm for H at the carbons 3 to 6. Furthermore, the peak at 3.61 ppm attributed to the H at the carbon 2, at 3.29 ppm for O-methylated group, at 3.02 ppm for quaternized amino group, at 2.83 ppm for dimethyl amino group and peak at 2.05 ppm (s, 3H) from the acetyl protons of the GluNAc units.

Figure 4.6h exhibited the ^{1}H NMR spectrum of 4-CBS-Chitosan Quat-188 was similar to that of Chitosan Quat-188 except the peaks at chemical shift at 7.91 ppm (d, 2H) and 7.86 ppm (d, 2H) were which due to the aromatic proton position of the sulfonamide ring.

Finally, the ^{1}H NMR spectrum of OA-4-CBS-TMC (Figure 4.6i) showed the characteristic peaks of both 4-CBS-TMC and oleoyl acid segments. The aromatic proton positions of the sulfonamide ring showed at 7.98 ppm (d, 2H) and 7.77 ppm (d, 2H). The peaks at 5.03 ppm for H at the carbon 1, at 4.34-3.74 ppm for H at the carbons 3 to 6, at 3.61 ppm for H at the carbon 2, at 3.28 ppm for O-methylated group, at 3.01 ppm for quaternized amino group, at 2.82 ppm for dimethyl amino group and peak at 2.02 ppm (s, 3H) from the acetyl protons of the GluNAc units. The proton positions of the long chain hydrocarbon showed at 5.27 ppm for H for -CH- (*i*), at 2.54 ppm for H for -CH$_2$CO- (*e*), at 1.96 ppm for H for CH$_2$CH- (*d*), at 1.54 ppm for H for -CH$_2$CH$_2$CO- (*c*), at 1.24 ppm for H for -CH$_2$- (*b*) and peak at 0.84 ppm for H for -CH$_3$ (*a*). These results support that the OA-4-CBS-TMC were successfully prepared.

Figure 4.6j exhibited the ^{1}H NMR spectrum of OA-4-CBS-Chitosan Quat-188 was similar to that of 4-CBS-Chitosan Quat-188 except the peaks at chemical shift at 5.17 ppm for H for -CH-(*i*), at 2.43 ppm for H for -CH$_2$CO- (*e*), at 1.92 ppm for H for CH$_2$CH-(*d*), at 1.43 ppm for H for -CH$_2$CH$_2$CO- (*c*), at 1.13 ppm for H for -CH$_2$- (*b*) and peak at 0.75 ppm for H for -CH$_3$ (*a*) which were due to the proton positions of the long chain hydrocarbon. These results support that the OA-4-CBS-Chitosan Quat-188 were successfully prepared.
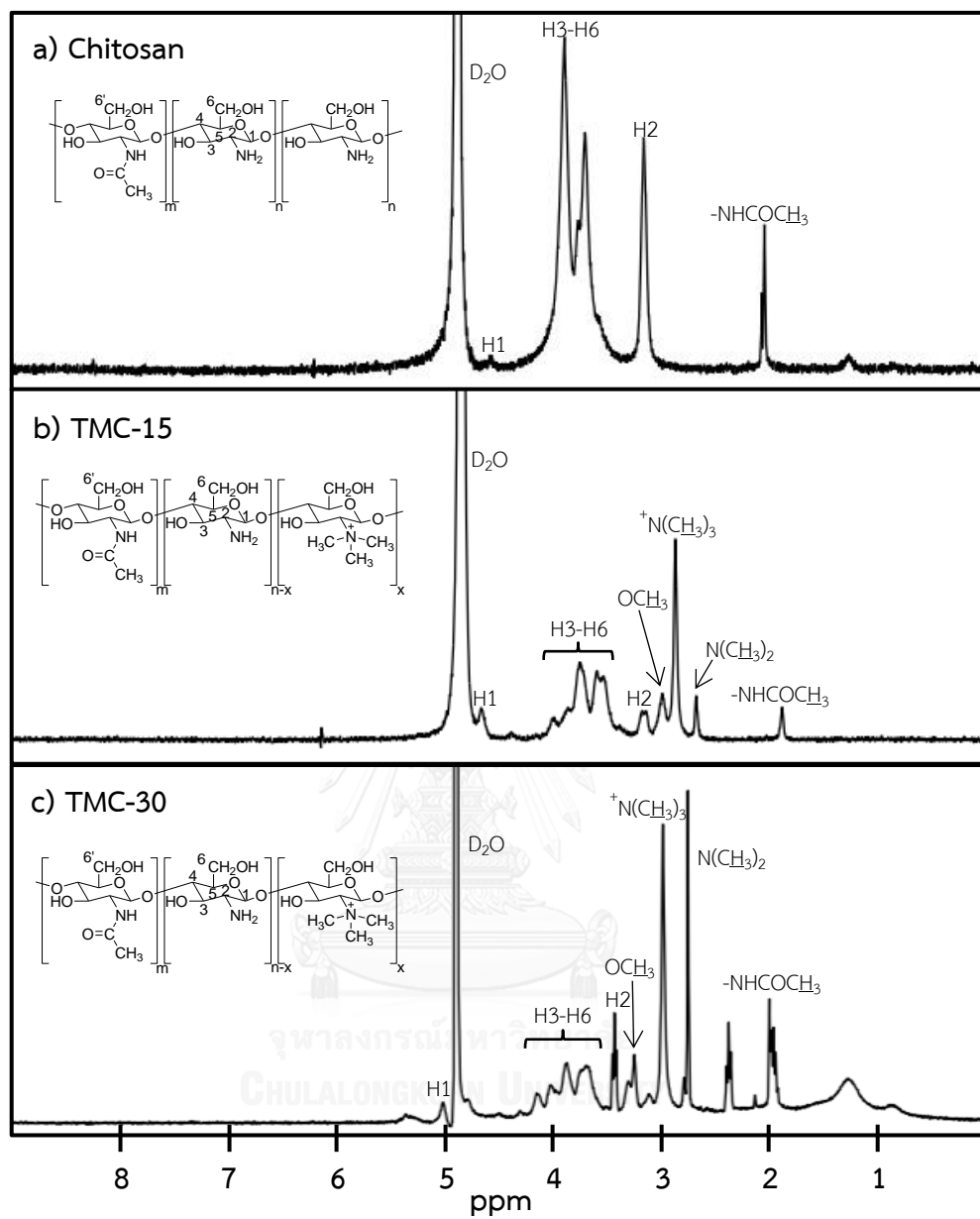
Figure 4.4 The ^{1}H NMR spectra of a) chitosan, b) TMC-15 and c) TMC-30
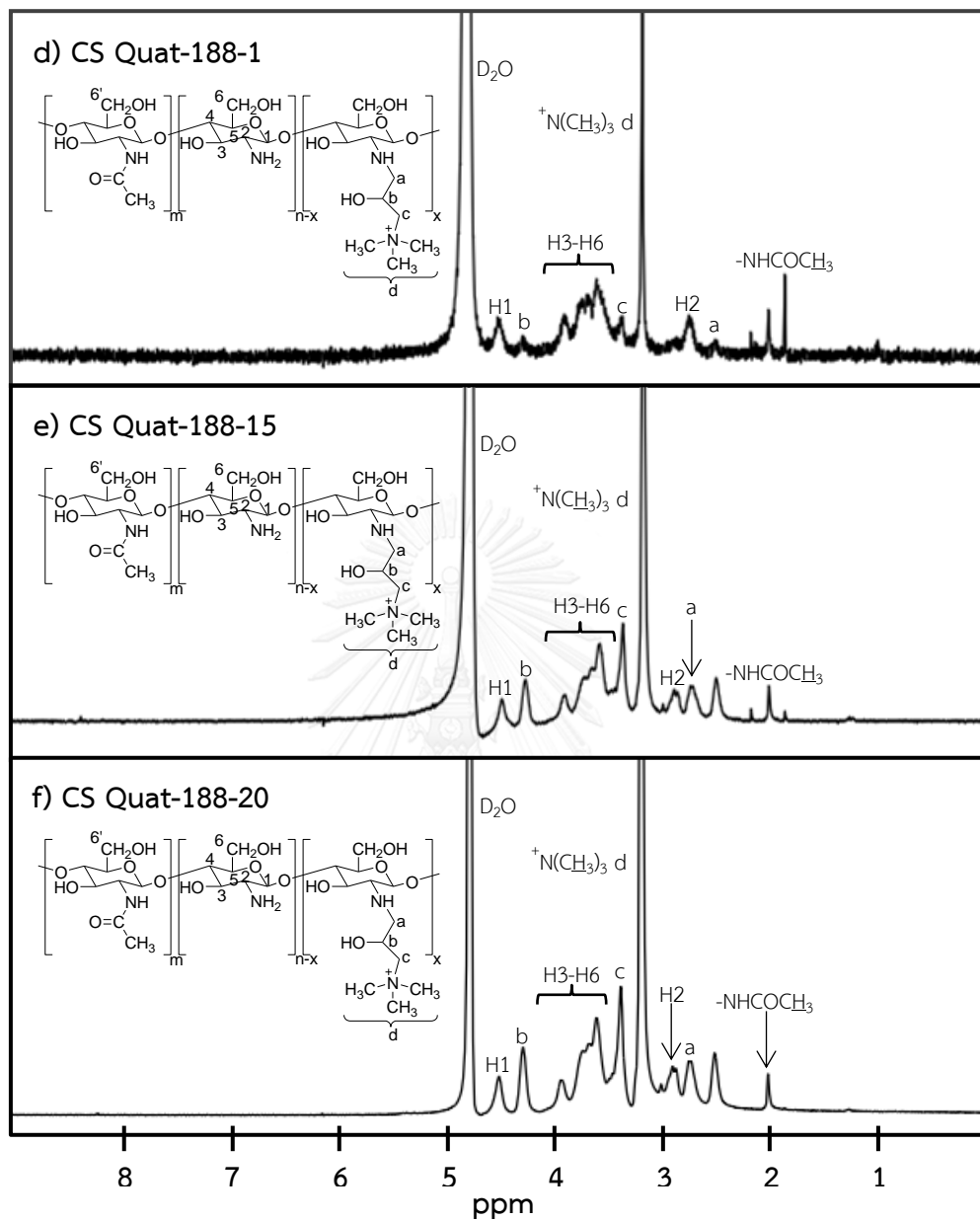
Figure 4.5 The ^{1}H NMR spectra of d) CS Quat-188-1, e) CS Quat-188-15 and f) CS Quat-188-20
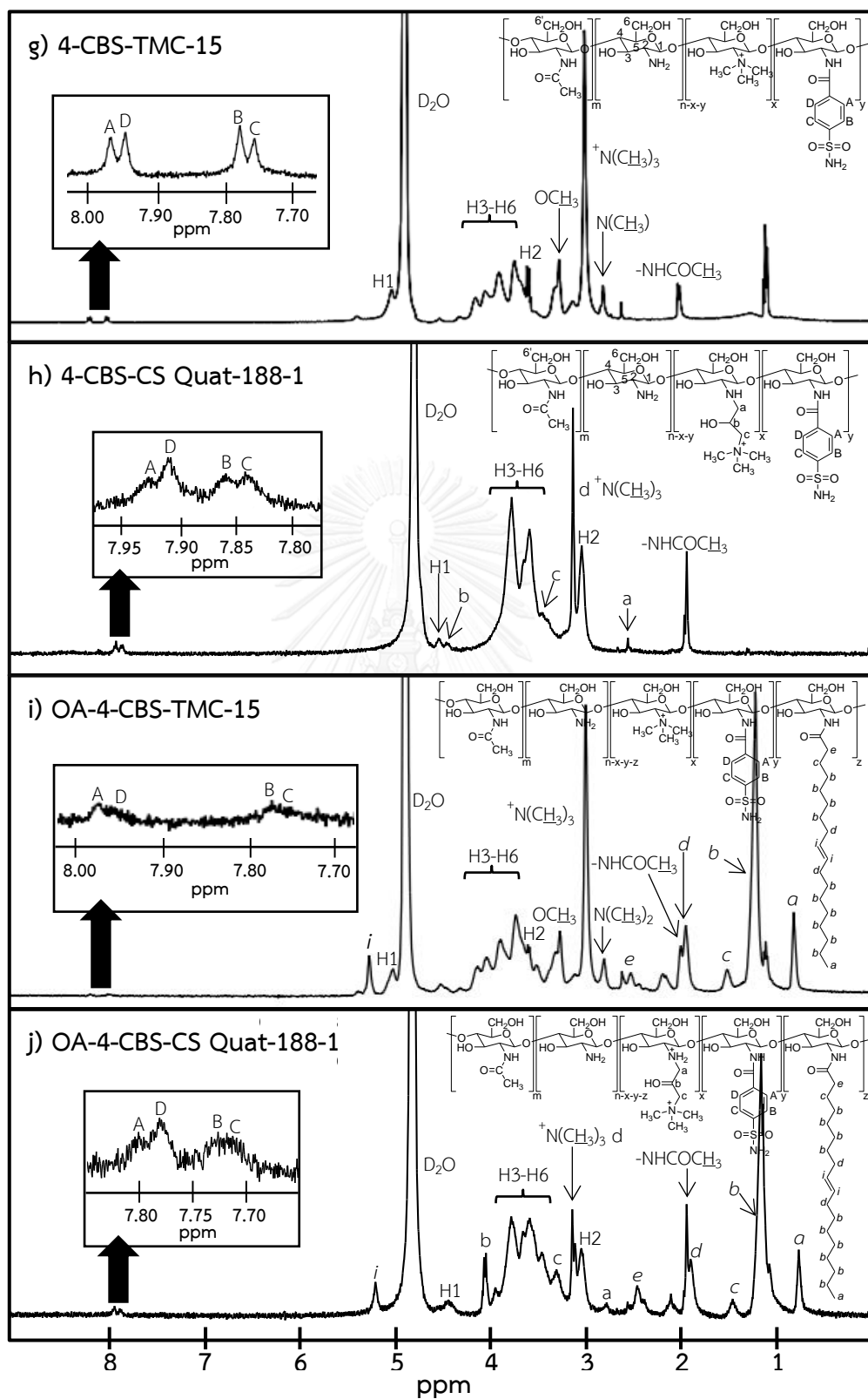
Figure 4.6 The ^{1}H NMR spectra of g) 4-CBS-TMC-15, h) 4-CBS-CS Quat-188-1, i) OA-4-CBS-TMC-15 and j) OA-4-CBS-CS Quat-188-1

4.2.3 The degree of quaternization (%DQ) and the degree of substitution (%DS)

The degree of quaternization (%DQ) of TMC and CS Quat-188, calculated from the equation (3) in section 3.3.2.3, were 18.90% and 24.05%, respectively. The degree of substitution (%DS) of 4-CBS on TMC, 4-CBS on CS Quat-188, OA on 4-CBS-TMC, and OA on 4-CBS-CS Quat-188 calculated from the equation (4) and (5) in section 3.3.2.3 were 9.70%, 10.36%, 34.15%, and 37.88%, respectively (Appendix A). Moreover, the degree of quaternization (%DQ) and the degree of substitution (%DS) have influence to develop structure for forming self-assembly together along with enhance the mucoadhesive properties of the chitosan due to the chemical structure influences the morphology of self-assembly.

4.3 *In vitro* bioadhesion of mucin to chitosan and the modified chitosan

4.3.1 Assessment of the mucoadhesive behavior of chitosan and the modified chitosan (TMC, CS Quat-188, 4-CBS-TMC, 4-CBS-CS Quat-188, OA-4-CBS-TMC, and OA-4-CBS-CS Quat-188) by mucin glycoprotein assay

Mucoadhesive governed the increased localization and residence time at the site of drug absorption. Moreover, it provided an intensified contact with the mucosa and, subsequently, increased the drug concentration gradient at the required site [14].

The mechanism of mucoadhesion has been theoretically reported to be based on the six general components of electrostatic, wetting, adsorption, diffusion, mechanical and fracture theories. Many methods have been employed to evaluate these interactions *in vitro* and *in vivo* [4, 84].

In this study, porcine mucin type II was selected which is typically used in mucoadhesion assays due to its lower batch-to-batch variability and higher between assay reproducibility. As a strong interaction exists between mucin and chitosan or its

derivatives, mucin should be spontaneously adsorbed onto the surface of the chitosan or its derivatives.

Periodic Acid Schiff (PAS) colorimetric method was used to qualify mucin conjugated polymer bioadhesived strength [42, 45] in the simulated gastrointestinal fluid in pH 1.2 (SGF) and pH 6.4 (SIF) that a strong interaction exists between mucin and chitosan or modified chitosan (TMC, CS Quat-188, 4-CBS-TMC, 4-CBS-CS Quat-188, OA-4-CBS-TMC, and OA-4-CBS-CS Quat-188). The mucin should be spontaneously adsorbed on the surface of the chitosan and modified chitosan. The mucoadhesive property of the chitosan and its derivatives was assessed by suspension of mucin in their aqueous solutions (in pH 1.2 and 6.4) at room temperature. The linearity range for mucin at the wavelength of detection at 555 nm was obtained as 0.1-0.5 mg/mL. The linear equations obtained by least square method were y = 0.0785x + 0.0011 and y = 0.398x + 0.0286 in pH 1.2 and 6.4, respectively (Appendix B).

4.3.2 Adsorption of mucin on polymer

The amount of mucin that was adsorped onto the polymer depend on ionization of sialic acid of the mucus glycoprotein and polymer that is to say the value of pK_a and pI for sialic acid and mucin are 2.6 and ~3-5, respectively [32]. Therefore the different forms of the glycoprotein will be influenced by the pH value of the environment [47].

Table 4.1 Comparison of chitosan and modified chitosan (TMC, CS Quat-188, 4-CBS-TMC, 4-CBS-CS Quat-188, OA-4-CBS-TMC, and OA-4-CBS-CS Quat-188) to mucoadhesive property

Sample	Adsorbed of mucin at pH1.2 (mg) (±SD, n=3)	Adsorbed of mucin at pH6.4 (mg) (±SD, n=3)
CS	0.111±0.003	0.216±0.007
TMC	0.124±0.003	0.240±0.006
4-CBS-TMC	0.149±0.001	0.255±0.005
OA-4-CBS-TMC	0.289±0.002	0.319±0.003
CS Quat-188	0.181±0.002	0.266±0.006
4-CBS-CS Quat-188	0.219±0.002	0.287±0.001
OA-4-CBS-CS Quat-188	0.339±0.002	0.389±0.009

The mucoadhesion of chitosan, TMC, CS Quat-188, 4-CBS-TMC, 4-CBS-CS Quat-188, OA-4-CBS-TMC, and OA-4-CBS-CS Quat-188 in simulated gastric fluid (SGF, pH 1.2) and simulated intestinal fluid (SIF, pH 6.4) were summarized in Table 4.1 and Figure 4.7. At pH 1.2 (SGF), chitosan showed an adsorption of mucin at 0.111 mg/mL, while TMC showed higher absorption of mucin (0.124 mg/mL) than that for chitosan. At pH1.2 (SGF), the amino groups ($-NH_2$) of chitosan backbone were partially protonated to the ammonium cation groups ($-NH_3^+$) because pK_a of chitosan was 6.5-6.8. It was not completely interact with negative charge of native mucin (pK_a = 2.6). When chitosan was quaternized and formed to TMC which increased permanently cationic charges site of chitosan and enhanced electrostatic interactions with negative charges ($-COO^-$ or $-SO_3^-$ groups) on mucin lead to increases the mucoadhesive properties. For CS Quat-188 showed higher absorption of mucin (0.181 mg/mL) than that for TMC because side chain of CS Quat-188 could form hydrogen

bonding with sialic acid (-COOH and -SO$_3$H groups) of the mucin glycoprotein apart from electrostatic interaction. In case of 4-CBS-TMC and 4-CBS-CS Quat-188 showed higher absorption of mucin (0.149 and 0.219 mg/mL, respectively) than that for quaternized chitosan. The mucoadhesive forces were likely to be dominated by electrostatic interactions and hydrophobic effects of the -CH$_3$ and aromatic part of 4-CBS groups on the polymer backbone that interact with the -CH$_3$ groups on the mucin side chains. Moreover, the hydroxyl and carbonyl end groups of side chain cloud form hydrogen bonding with sialic acid (-COOH and -SO$_3$H groups) on the mucin lead to increase the mucoadhesive properties. For OA-4-CBS-TMC and OA-4-CBS-CS Quat-188 showed absorption of mucin at 0.289 and 0.339 mg/mL, respectively. They displayed higher mucoadhesive properties than 4-CBS-QCS. As very high content of OA substituent increased the hydrophobic part, the mucoadhesive properties increases. Therefore, the mucoadhesion is typically related to the mucoadhesive force between the interacting polymer and mucin.

At pH 6.4 (SIF), all polymers showed higher adsorption of mucin than that for all polymers at pH 1.2. Because at pH 6.4 (SIF), the cysteine-rich (-SH) subdomains of the mucin glycoprotein was deprotonated and increased concentration of the reactive form of thiolate anions, (-S$^-$, pK_a = 2.6). The mucoadhesive properties increase due to enhance electrostatic interaction between cationic charges site of chitosan and negative charges (-COO$^-$, -SO$_3^-$, and -S$^-$ groups) on mucin. Therefore, the effect of hydrogen bonding and hydrophobic impact on the mucoadhesion of chitosan, TMC, CS Quat-188, 4-CBS-TMC, 4-CBS-CS Quat-188, OA-4-CBS-TMC, and OA-4-CBS-CS Quat-188 in higher pH range.
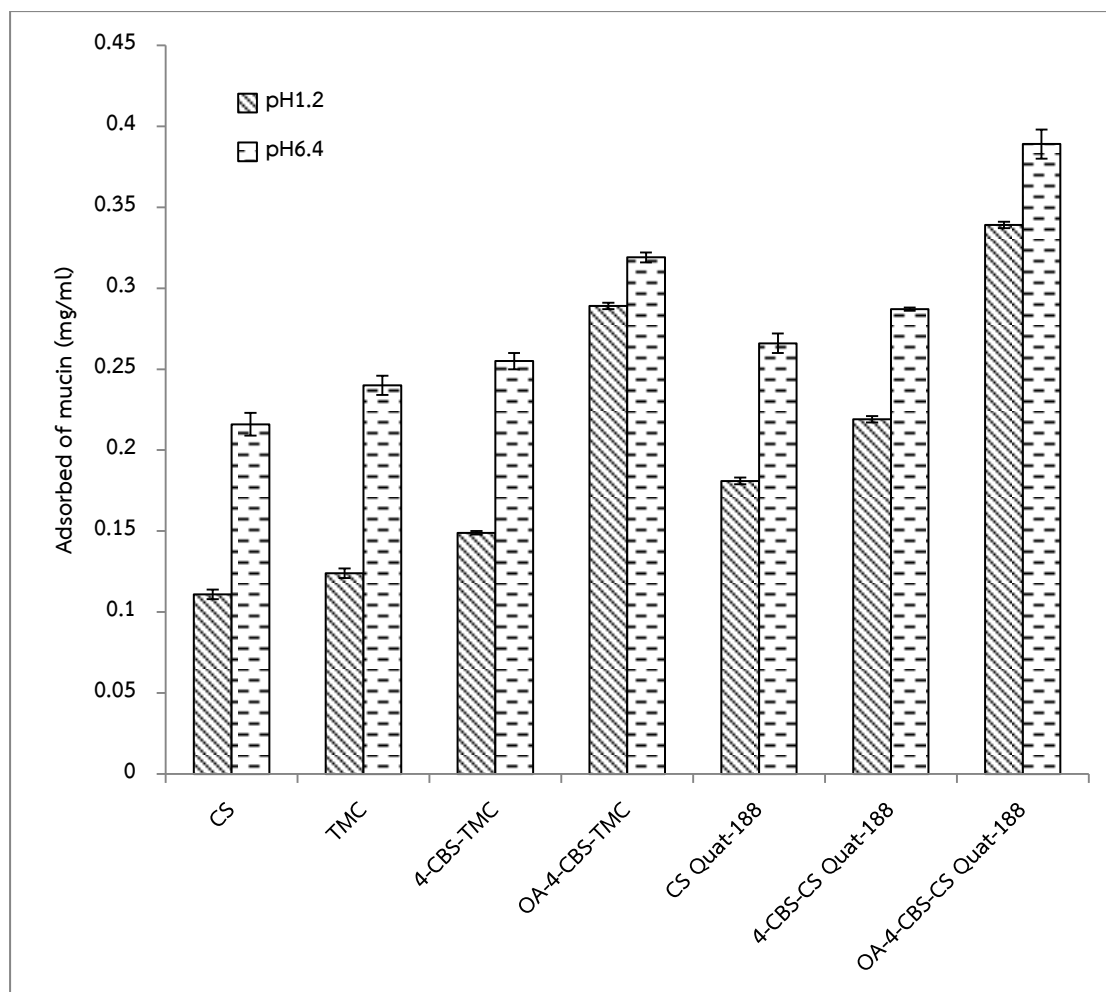
Figure 4.7 Adsorption of mucin on chitosan and modified chitosan (TMC, CS Quat-188, 4-CBS-TMC, 4-CBS-CS Quat-188, OA-4-CBS-TMC, and OA-4-CBS-CS Quat-188) at pH 1.2 and 6.4. Data are shown as the mean±SD and derived from three independent repeats.

4.4 Self-assembly Morphologies

Factors that can control molecular structure assembly include pH, solvents, co-assembly molecules, temperature and re-dispersed concentration. In this study, for the self-assembly of OA-4-CBS-TMC and OA-4-CBS-CS Quat-188 molecules, re-dispersion concentration ranging from 0.3 to 4.3 mg/mL in distilled water were first considered to control the fabrication of fractal hyperbranch structure. The molecular design of the OA-4-CBS-TMC and OA-4-CBS-CS Quat-188 is shown in Figure 4.8 [85].

a)

b)
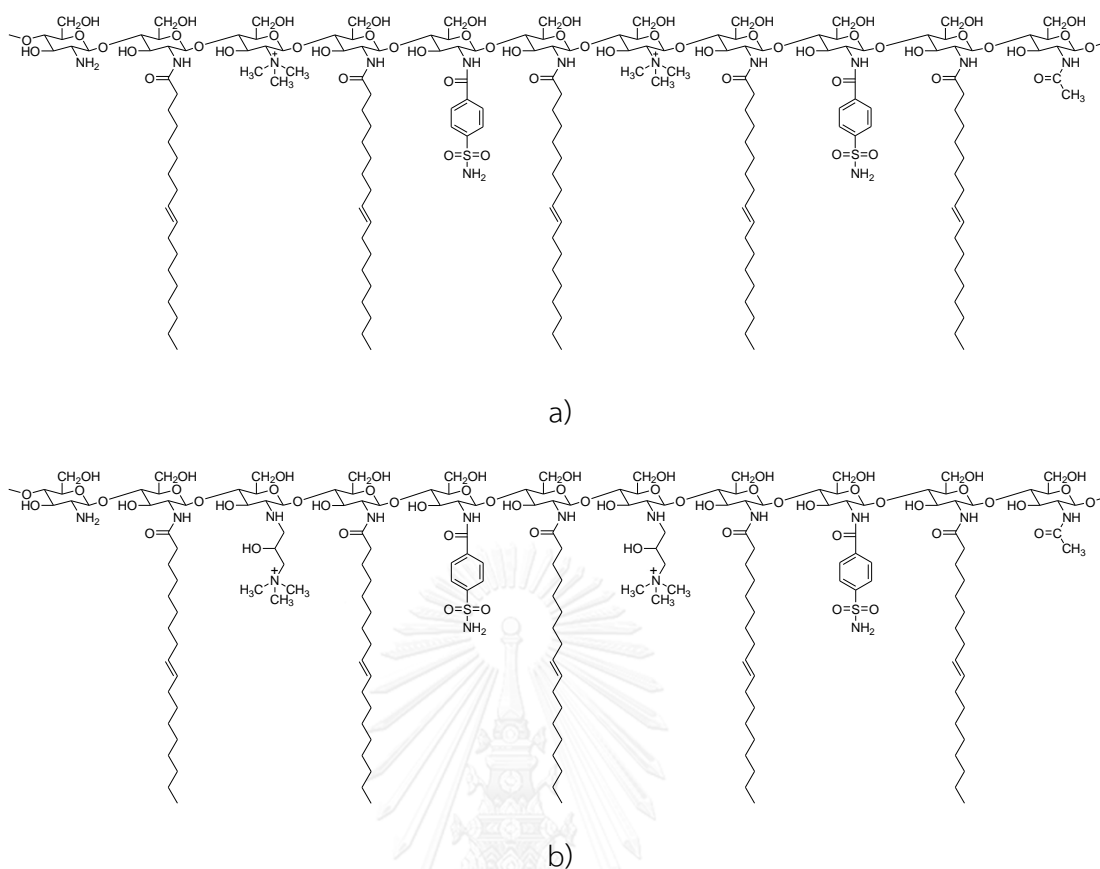
Figure 4.8 The molecular structures of a) OA-4-CBS-TMC and b) OA-4-CBS-CS Quat-188

Figure 4.8 displays the chemical structure of one OA-4-CBS-TMC and OA-4-CBS-CS Quat-188 molecule, incorporating the four key structural features: the 4-CBS substituent, $-N^+(CH_3)_3$ of the quaternized chitosan, OA hydrophobic tail and the chitosan backbone. The first key component, the aromatic 4-CBS substituent, induced π-π aromatic stacking interaction between small aromatic rings and allowed the formation of well-ordered fractal hyperbranch structure. These interactions provided discrete nanostructures due to the extremely rigid characteristic of the nanofractal hyperbranches when re-dispersed in distilled water. The second key component, the quaternized chitosan $-N^+(CH_3)_3$ enhanced the nanofractal hyperbranches solubility in water without altering the pH [86]. Therefore, pH is a critical factor for generating successful self-assembled nanofractal hyperbranches. The third key component was the inclusion of various hydrophobic tails with

different alkyl lengths, such as oleic acid, cholesterol, linoleic acid, and stearic acid [31, 87], to assemble the nanofractal hyperbranches. OA served one of the most important roles for designing this molecular feature. OA contains hydrophobic regions to control the self-assembly of amphiphiles by shielding the ampliphiles from water to create 4-CBS and -N$^+$(CH$_3$)$_3$ signals on the nanofractal hyperbranches periphery. The last key component, the chitosan backbone, formed intramolecular hydrogen bonds, which led to further enhanced horizontal molecular packing at both very low and high polymer dispersed concentrations. Therefore, intermolecular hydrogen bonding caused the connection of OA-4-CBS-TMC and OA-4-CBS-CS Quat-188 nanofractal hyperbranches, one factor for molecular packing. Utilizing these key factors, nanofractal hyperbranches were fabricated in water. The hydrophobic core of the OA substitution was buried within the structure such that it did not contact water, whereas the hydrophilic segments, such as -N$^+$(CH$_3$)$_3$ of the chitosan backbone and the 4-CBS substituent, surrounded the OA core and resided adjacent to the water phase. The driving forces of aromatic 4-CBS stacking, hydrogen bonding along the chitosan backbone, the hydrophobic interactions of the alkyl OA tails and the electrostatic repulsion of -N$^+$(CH$_3$)$_3$ enhanced the nanocubes formation and facilitated the self-assembly of OA-4-CBS-TMC and OA-4-CBS-CS Quat-188 nanofractal hyperbranches. The aromatic 4-CBS stacking, hydrogen bonding along the chitosan backbone, and the hydrophobic interactions of the alkyl OA tails were attraction forces that promoted the aggregation of OA-4-CBS-TMC and OA-4-CBS-CS Quat-188, whereas the -N$^+$(CH$_3$)$_3$ was the charged component that promoted the dissociation of OA-4-CBS-TMC and OA-4-CBS-CS Quat-188. As the molecular-level packing progressed, which depended on a delicate balance of energy contribution, the morphological and structural features, including length, packing density, and order of surface nanofractal hyperbranches were revealed.

0.3 mg/mL

1.3 mg/mL

More

2.3 mg/mL

a)

Aggregates of self-assembly

Separate particles
on substrate

Time

Primitive self-assembly

Time

Self-assembly association

Different morphologies
(Depend on re-dispersed
concentration)

b)
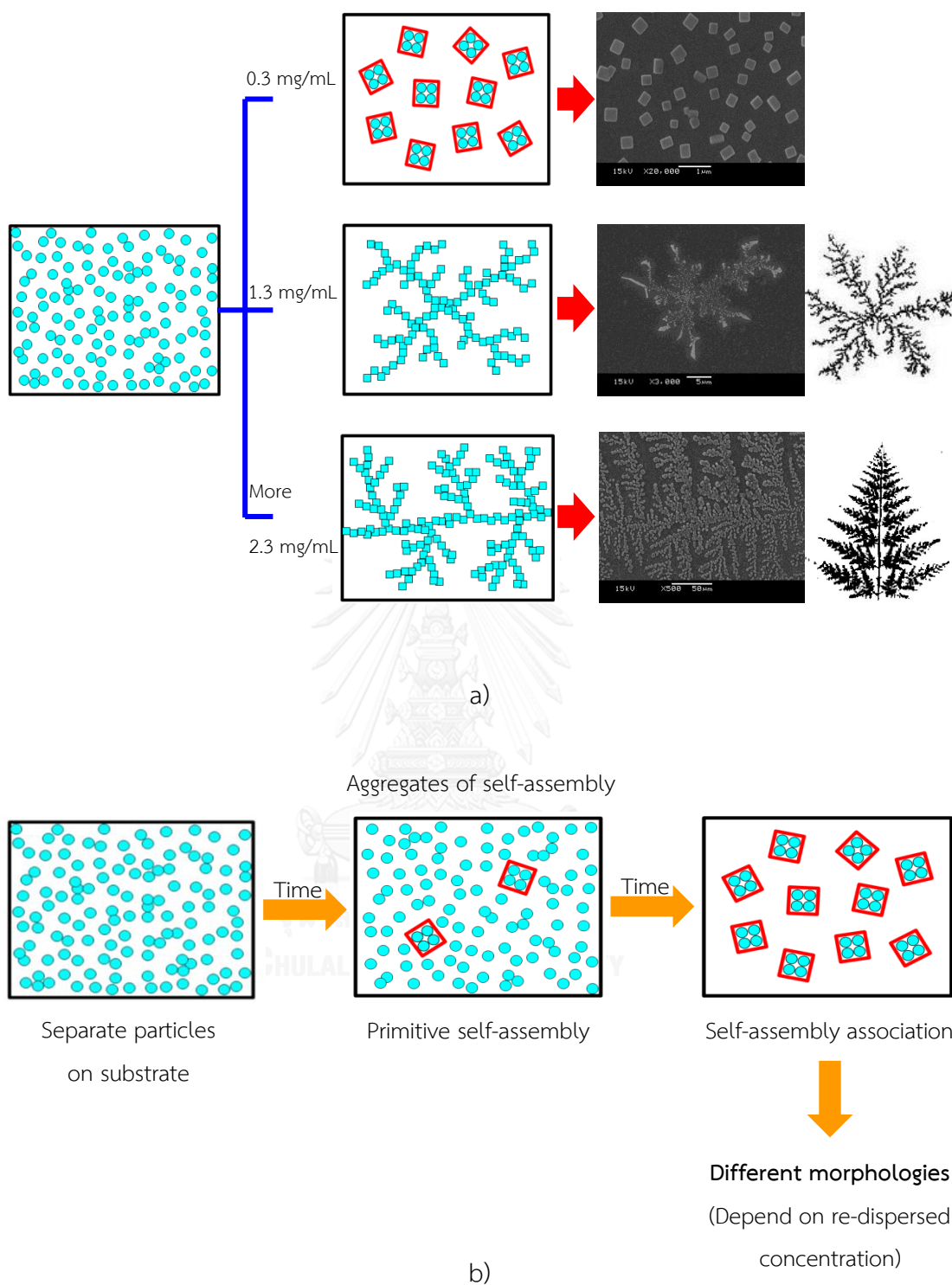
Figure 4.9 a) A schematic phase diagram of OA-4-CBS-QCS assemblies, which are dependent on concentration in distilled water, ranging from 0.3 to 4.3 mg/mL [27]. b) The formation stages of OA-4-CBS-QCS particles dependent on re-dispersion in distilled water.

In this study, for the self-assembly of OA-4-CBS-TMC and OA-4-CBS-CS Quat-188 molecules, re-dispersion concentration ranging from 0.3 to 4.3 mg/mL in distilled water were first considered to control the fabrication of nanofractal hyperbranches (Figure 4.9a). As shown in Figure 4.9b), in the early stages, while the OA-4-CBS-TMC and OA-4-CBS-CS Quat-188 particles were dispersed in distilled water, the peripheral chitosan backbone was separated. Next, the particles gradually swelled, resulting in aggregation due to the random walk process [27, 88], and became primitively self-assembled. This process allowed an alteration in self-assembly structure in response to changing the concentration of OA-4-CBS-TMC and OA-4-CBS-CS Quat-188 in distilled water. The final nanofractal hyperbranch shape, size, and self-assembled stability expressed an optimum thermodynamic state, which was characterized by a combination of factors, such as chain stretching, interfacial tension, and intercoronal chain interaction. The excellent long term stability of various morphologies dispersed in distilled water could be determined by re-observation by SEM. Although the self-assembly of a spherical geometry was quite general, other morphologies, such as nanocubes, nanohyperbranches, and nanofractal hyperbranches, were observed at different re-dispersion concentrations. All of morphologies were not change in shape and size over time.

4.4.1 Cubic structure

At a low concentration (0.3 mg/mL), the morphologies of OA-4-CBS-TMC and OA-4-CBS-CS Quat-188 structures included nanocubes (Figure 4.10). The relative stability of the various possible packing self-assemblies was believed to be primarily controlled by the balance of three energies: chain stretching, interfacial tension, and intercoronal chain interactions. When the concentration was low, the amount of OA-4-CBS-TMC and OA-4-CBS-CS Quat-188 were too low to provide the high intercoronal chain repulsion of $-N^+(CH_3)_3$ on the surface. The OA-4-CBS-TMC and OA-4-CBS-CS Quat-188 structure were determined by a delicate balance of forces operating at the interfacial region of the 4-CBS and $-N^+(CH_3)_3$ groups and within the hydrophobic core of aggregated OA, inducing a spherical shape. However, the formation of OA-4-CBS-

TMC and OA-4-CBS-CS Quat-188 into spheres could not continue indefinitely because the stretching energy due to the entropy of OA. Consequently, the high stretching energy would begin to induce ordered and arranged themselves into a roughly cubic lattice instead of spheres to reduce the thermodynamic penalty of chain stretching with a width on the order of ≈200-300 nm. These results probably related with the repulsive interaction between positive charges of quaternized chitocan, which probably play a very important role during the formation of cubic lattice (Figure 4.10). The proposed self-assembly process of the nanocubes can explain that the quaternary amino group of the chitosan backbone and the sulfonamide group of 4-CBS provided cation-dipole interaction.
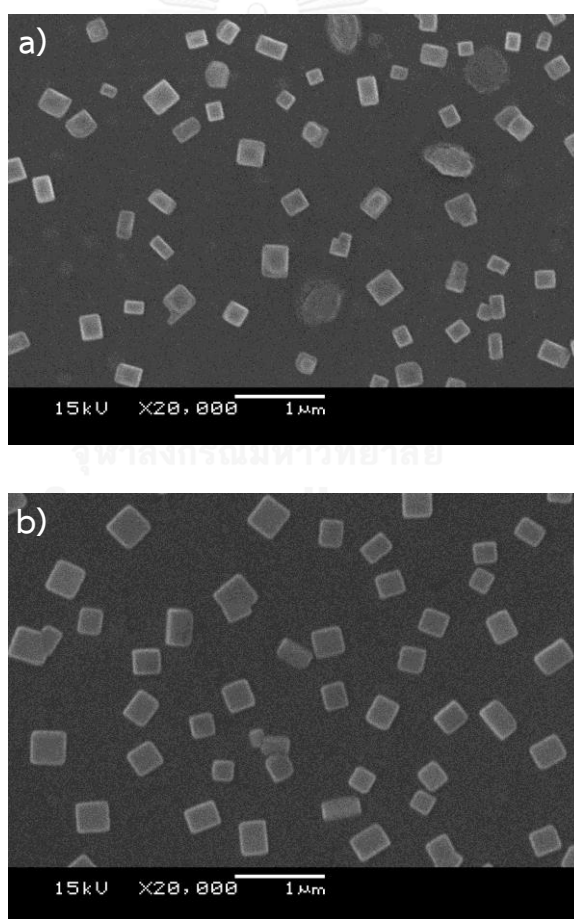

Figure 4.10 The morphologies of a) OA-4-CBS-TMC and b) OA-4-CBS-CS Quat-188 at low concentration (0.3 mg/mL).

4.4.2 Hyperbranch or fractal hyperbranch structure

Hyperbranch or fractal hyperbranch structure shown in Figure 4.11 was able to be formed at concentrations of 1.3, 2.3, and 3.3 mg/mL. The formation of the structure began as the aggregation of many nuclei, a state of lower free energy [89]. The concept of diffusion-limited aggregation (DLA), or the irreversible aggregation of small particles into clusters, has been previously developed [90]. The DLA concept received significant attention because it was a fundamental model for pattern growth and provided a basic understanding of complex aggregate formation of different shapes [91]. The model assumed that particles originate far from a developing immobile structure and undergo a random walk in their surrounding space. The particles stick to an existing structure when encountered. Therefore, the aggregated nuclei of OA-4-CBS-TMC and OA-4-CBS-CS Quat-188 became part of the primitive self-assembly that led to the formation of extremely complicated multi-branches. These branches grew from the central nucleus and were composed of nanofractal hyperbranches. Moreover, these branches repelled each other due to the repulsive positive charge of the $-N^+(CH_3)_3$ group. Generally, a hyperbranch structure formed and grew rapidly at the ends of the self-assembly rather than from other perimeter sites because the perimeter sites near the center were occluded [92]. The angles between the main and side branches, considered from the center outward, do not have fixed values. The widths of the branches were much narrower compared to the total length of each branch. Moreover, the branches were formed with a uniform width. When a branch reached a certain width, it split to generate new branches, and both the parent branch and the new branches continued to proliferate. This pattern generated largest diameter of approximately 2-9 µm. Thus nanofractal hyperbranched self-assembly of OA-4-CBS-TMC and OA-4-CBS-CS Quat-188 at high concentrations were successfully prepared.

At very high concentration (4.3 mg/mL), the space between polymeric units was very limited (Figure 4.11g and h). The concentration promoted growth onto functionalized interfaces. The nanofractal hyperbranches did not have enough space

to permit facile growth. Therefore, the high polymer content induced aggregation into thin films.
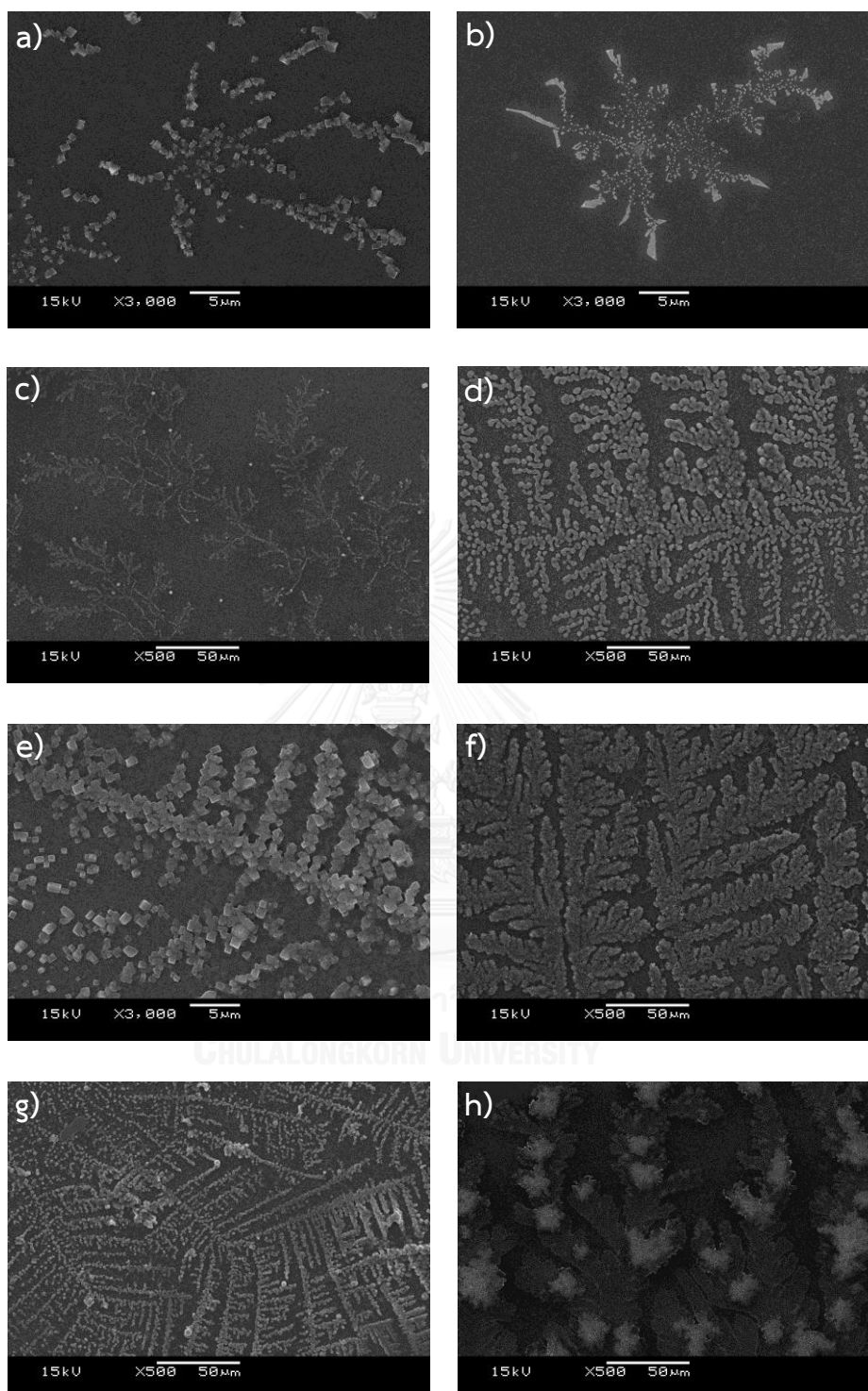
Figure 4.11 The morphologies of a) OA-4-CBS-TMC at 1.3 mg/mL, b) OA-4-CBS-CS Quat-188 at 1.3 mg/mL, c) OA-4-CBS-TMC at 2.3 mg/mL, d) OA-4-CBS-CS Quat-188 at 2.3 mg/mL, e) OA-4-CBS-TMC at 3.3 mg/mL, f) OA-4-CBS-CS Quat-188 at 3.3 mg/mL, g) OA-4-CBS-TMC at 4.3 mg/mL, and h) OA-4-CBS-CS Quat-188 at 4.3 mg/mL.

CHAPTER V
CONCLUSION AND SUGGESTION

5.1 Conclusion

In the present study, quaternized chitosan was synthesized to form TMC by methyl iodide and to form CS Quat-188 by *N*-(3-chloro-2-hydroxy-propyl) trimethylammonium chloride which reacted with the primary amino groups of chitosan and then 4-CBS and OA were covalently reacted at the primary amino groups of chitosan using EDAC as a coupling reagent. The degree of quaternization (%DQ) of TMC and CS Quat-188 and the degree of substitution (%DS) of 4-CBS on TMC, 4-CBS on CS Quat-188, OA on 4-CBS-TMC, and OA on 4-CBS-CS Quat-188 were calculated about 18.90%, 24.05%, 9.70%, 10.36%, 34.15%, and 37.88%, respectively by ^{1}H NMR, resulted in strongly improved mucoadhesive properties.

The mucoadhesiveness was determined by Periodic Acid Schiff (PAS) colorimetric method which was used to qualify mucin-conjugated polymer bioadhesived strength in the simulated gastrointestinal fluid (pH1.2 and 6.4). The obtained all polymers at pH 6.4 (SIF) showed highest mucoadhesive propoties.

Self-assembled OA-4-CBS-TMC and OA-4-CBS-CS Quat-188 nanofractal hyperbranches were successfully fabricated by only re-dispersing the compound in distilled water at concentration 2.3 and 3.3 mg/mL which were easy and stable one stop procedure. The nanofractal hyperbranches assembly relied interactions between the hydrophobic effect of OA, the aromatic stacking of 4-CBS, the electrostatic interactions of -N^{+}(CH$_3$)$_3$, and the hydrogen bonding of chitosan backbone. Moreover, they exhibited the highest mucoadhesion in phosphate buffer (PB, pH 6.4) compared to native chitosan due to high content of OA substituent to provide hydrophobic interaction with mucous membrane.

Therefore, the mucoadhesive OA-4-CBS-TMC and OA-4-CBS-CS Quat-188 nanofractal hyperbranches were suitable polymer for applying as drug carrier.

5.2 Suggestions for the future work

Develop the mucoadhesive self-assembled drug carrier for hydrophobic drug delivery in gastrointestinal tract in order to provide high content of drug encapsulation and prolong the residence time of intend drug at the site of absorption.

REFERENCES

[1]   Grabovac, V., Guggi, D., and Bernkop-Schnürch, A. Comparison of the mucoadhesive properties of various polymers. <u>Advanced Drug Delivery Reviews</u> 57(11) (2005): 1713-1723.

[2]   Ludwig, A. The use of mucoadhesive polymers in ocular drug delivery. <u>Advanced Drug Delivery Reviews</u> 57(11) (2005): 1595-1639.

[3]   Ugwoke, M.I., Agu, R.U., Verbeke, N., and Kinget, R. Nasal mucoadhesive drug delivery: Background, applications, trends and future perspectives. <u>Advanced Drug Delivery Reviews</u> 57(11) (2005): 1640-1665.

[4]   Mythri .G, K.K., M. Rupesh Kumar, Sd. Jagadeesh Singh. Novel Mucoadhesive Polymers –A Review. <u>Journal of Applied Pharmaceutical Science</u> 1(8) (2011): 37-42.

[5]   Bernkop-Schnürch, A., Kast, C.E., and Guggi, D. Permeation enhancing polymers in oral delivery of hydrophilic macromolecules: thiomer/GSH systems. <u>Journal of Controlled Release</u> 93(2) (2003): 95-103.

[6]   S.K.Tilloo, T.M.R., V.V.Kale. MUCOADHESIVE MICROPARTICULATE DRUG DELIVERY SYSTEM. <u>International Journal of Pharmaceutical Sciences Review and Research</u> 9(1) (2011): 52-56.

[7]   Riva, R., Ragelle, H., des Rieux, A., Duhem, N., Jérôme, C., and Préat, V. Chitosan and Chitosan Derivatives in Drug Delivery and Tissue Engineering. in Jayakumar, R., Prabaharan, M., and Muzzarelli, R.A.A. (eds.),<u>Chitosan for Biomaterials II</u>, pp. 19-44: Springer Berlin Heidelberg, 2011.

[8]   Lehr, C.-M., Bouwstra, J.A., Schacht, E.H., and Junginger, H.E. In vitro evaluation of mucoadhesive properties of chitosan and some other natural polymers. <u>International Journal of Pharmaceutics</u> 78(1–3) (1992): 43-48.

[9]   Shalini Mishra , G.K., P. Kothiyal. Formulation and Evaluation of Buccal Patches of Simvastatin by Using Different Polymers. <u>Journal of Pharmaceutical Innovation</u> 1 (2012): 87-92.

[10]   Kumar, M.N., Muzzarelli, R.A., Muzzarelli, C., Sashiwa, H., and Domb, A.J. Chitosan chemistry and pharmaceutical perspectives. Chem Rev 104(12) (2004): 6017-84.

[11]   Sinha, V.R., et al. Chitosan microspheres as a potential carrier for drugs. International Journal of Pharmaceutics 274(1–2) (2004): 1-33.

[12]   He, P., Davis, S.S., and Illum, L. In vitro evaluation of the mucoadhesive properties of chitosan microspheres. International Journal of Pharmaceutics 166(1) (1998): 75-88.

[13]   Vipin Bansal, P.K.S., Nitin Sharma, Om Prakash Pal and Rishabha Malviya. Applications of Chitosan and Chitosan Derivatives in Drug Delivery. Advances in Biological Research 5(1) (2011): 28-37.

[14]   Snyman, D., Hamman, J.H., and Kotze, A.F. Evaluation of the mucoadhesive properties of N-trimethyl chitosan chloride. Drug Dev Ind Pharm 29(1) (2003): 61-9.

[15]   Smart, J.D., Kellaway, I.W., and Worthington, H.E. An in-vitro investigation of mucosa-adhesive materials for use in controlled drug delivery. J Pharm Pharmacol 36(5) (1984): 295-9.

[16]   Nagarwal, R.C., Singh, P.N., Kant, S., Maiti, P., and Pandit, J.K. Chitosan nanoparticles of 5-fluorouracil for ophthalmic delivery: characterization, in-vitro and in-vivo study. Chem Pharm Bull (Tokyo) 59(2) (2011): 272-8.

[17]   Dhawan, S., Singla, A.K., and Sinha, V.R. Evaluation of mucoadhesive properties of chitosan microspheres prepared by different methods. AAPS PharmSciTech 5(4) (2004): e67.

[18]   Sogias, I.A., Williams, A.C., and Khutoryanskiy, V.V. Why is chitosan mucoadhesive? Biomacromolecules 9(7) (2008): 1837-42.

[19]   Bernkop-Schnürch, A. and Dünnhaupt, S. Chitosan-based drug delivery systems. European Journal of Pharmaceutics and Biopharmaceutics 81(3) (2012): 463-469.

[20]   Dash, M., Chiellini, F., Ottenbrite, R.M., and Chiellini, E. Chitosan—A versatile semi-synthetic polymer in biomedical applications. Progress in Polymer Science 36(8) (2011): 981-1014.

[21] Mourya, V.K. and Inamdar, N.N. Chitosan-modifications and applications: Opportunities galore. Reactive and Functional Polymers 68(6) (2008): 1013-1051.

[22] Sieval, A.B., Thanou, M., Kotze´, A.F., Verhoef, J.C., Brussee, J., and Junginger, H.E. Preparation and NMR characterization of highly substituted N-trimethyl chitosan chloride. Carbohydrate Polymers 36(2) (1998): 157-165.

[23] Thanou, M.M., et al. Effect of degree of quaternization of N-trimethyl chitosan chloride for enhanced transport of hydrophilic compounds across intestinal caco-2 cell monolayers. J Control Release 64(1-3) (2000): 15-25.

[24] Sajomsang, W., Tantayanon, S., Tangpasuthadol, V., and Daly, W.H. Quaternization of N-aryl chitosan derivatives: synthesis, characterization, and antibacterial activity. Carbohydr Res 344(18) (2009): 2502-11.

[25] Suvannasara, P., Juntapram, K., Praphairaksit, N., Siralertmukul, K., and Muangsin, N. Mucoadhesive 4-carboxybenzenesulfonamide-chitosan with antibacterial properties. Carbohydrate Polymers 94(1) (2013): 244-252.

[26] Suvannasara, P., Siralertmukul, K., and Muangsin, N. Electrosprayed 4-carboxybenzenesulfonamide-chitosan microspheres for acetazolamide delivery. Int J Biol Macromol 64 (2014): 240-6.

[27] Hu, Y., et al. Self-assembly and Fractal Feature of Chitosan and Its Conjugate with Metal Ions: Cu (II)/Ag (I). International Journal of Molecular Sciences 8(1) (2007): 1-12.

[28] Gao, C. and Yan, D. Hyperbranched polymers: from synthesis to applications. Progress in Polymer Science 29(3) (2004): 183-275.

[29] Havlin, S., et al. Fractals in biology and medicine. Chaos Solitons Fractals 6 (1995): 171-201.

[30] Rösler, A., Vandermeulen, G.W.M., and Klok, H.-A. Advanced drug delivery devices via self-assembly of amphiphilic block copolymers. Advanced Drug Delivery Reviews 64, Supplement(0) (2012): 270-279.

[31] Park, J.H., Saravanakumar, G., Kim, K., and Kwon, I.C. Targeted delivery of low molecular drugs using chitosan and its derivatives. Advanced Drug Delivery Reviews 62(1) (2010): 28-41.

[32]   Palmer, L.C. and Stupp, S.I. Molecular Self-Assembly into One-Dimensional Nanostructures. Accounts of chemical research 41(12) (2008): 1674-1684.

[33]   Van Tomme, S.R., Mens, A., van Nostrum, C.F., and Hennink, W.E. Macroscopic hydrogels by self-assembly of oligolactate-grafted dextran microspheres. Biomacromolecules 9(1) (2008): 158-65.

[34]   Hartgerink, J.D., Beniash, E., and Stupp, S.I. Self-Assembly and Mineralization of Peptide-Amphiphile Nanofibers. Science 294(5547) (2001): 1684-1688.

[35]   Gu, J.M., Robinson, J.R., and Leung, S.H. Binding of acrylic polymers to mucin/epithelial surfaces: structure-property relationships. Crit Rev Ther Drug Carrier Syst 5(1) (1988): 21-67.

[36]   Good, W.R. Transder®-Nitro Controlled Delivery of Nitroglycerin via the Transdermal Route. Drug Development and Industrial Pharmacy 9(4) (1983): 647-670.

[37]   Thornton, D.J. and Sheehan, J.K. From mucins to mucus: toward a more coherent understanding of this essential barrier. Proc Am Thorac Soc 1(1) (2004): 54-61.

[38]   Carlstedt, I. and Sheehan, J.K. Structure and macromolecular properties of cervical mucus glycoproteins. Symp Soc Exp Biol 43 (1989): 289-316.

[39]   Allen, A., Cunliffe, W.J., Pearson, J.P., and Venables, C.W. The adherent gastric mucus gel barrier in man and changes in peptic ulceration. Journal of Internal Medicine 228(S732) (1990): 83-90.

[40]   Kerss, S., Allen, A., and Garner, A. A simple method for measuring thickness of the mucus gel layer adherent to rat, frog and human gastric mucosa: influence of feeding, prostaglandin, N-acetylcysteine and other agents. Clin Sci (Lond) 63(2) (1982): 187-95.

[41]   Sonju, T., Christensen, T.B., Kornstad, L., and Rolla, G. Electron microscopy, carbohydrate analyses and biological activities of the proteins adsorbed in two hours to tooth surfaces in vivo. Caries Res 8(2) (1974): 113-22.

[42]   Carvalho, F.C., Bruschi, M.L., Evangelista, R.C., and Gremião, M.P.D. Mucoadhesive drug delivery systems. Brazilian Journal of Pharmaceutical Sciences 46 (2010): 1-17.

[43]   Peppas, N.A. and Sahlin, J.J. Hydrogels as mucoadhesive and bioadhesive materials: a review. Biomaterials 17(16) (1996): 1553-1561.

[44]   Ponchel, G., Touchard, F., Duchêne, D., and Peppas, N.A. Bioadhesive analysis of controlled-release systems. I. Fracture and interpenetration analysis in poly(acrylic acid)-containing systems. Journal of Controlled Release 5(2) (1987): 129-141.

[45]   Kinloch, A.J. The science of adhesion. Journal of Materials Science 15(9) (1980): 2141-2166.

[46]   Jiménez-castellanos, M.R., Zia, H., and Rhodes, C.T. Mucoadhesive Drug Delivery Systems. Drug Development and Industrial Pharmacy 19(1-2) (1993): 143-194.

[47]   Smart, J.D. The basics and underlying mechanisms of mucoadhesion. Advanced Drug Delivery Reviews 57(11) (2005): 1556-1568.

[48]   Ahuja, A., Khar, R.K., and Ali, J. Mucoadhesive Drug Delivery Systems. Drug Development and Industrial Pharmacy 23(5) (1997): 489-515.

[49]   Dubolazov, A.V., Nurkeeva, Z.S., Mun, G.A., and Khutoryanskiy, V.V. Design of Mucoadhesive Polymeric Films Based on Blends of Poly(acrylic acid) and (Hydroxypropyl)cellulose. Biomacromolecules 7(5) (2006): 1637-1643.

[50]   Kim, T.H., Ahn, J.S., Choi, H.K., Choi, Y.J., and Cho, C.S. A novel mucoadhesive polymer film composed of carbopol, poloxamer and hydroxypropylmethylcellulose. Arch Pharm Res 30(3) (2007): 381-6.

[51]   Keely, S., et al. In Vitro and ex Vivo Intestinal Tissue Models to Measure Mucoadhesion of Poly (Methacrylate) and N-Trimethylated Chitosan Polymers. Pharmaceutical Research 22(1) (2005): 38-49.

[52]   Lim, S.T., Martin, G.P., Berry, D.J., and Brown, M.B. Preparation and evaluation of the in vitro drug release properties and mucoadhesion of novel microspheres of hyaluronic acid and chitosan. Journal of Controlled Release 66(2–3) (2000): 281-292.

[53]   Bernkop-Schnürch, A., Schwarz, V., and Steininger, S. Polymers with Thiol Groups: A New Generation of Mucoadhesive Polymers? Pharmaceutical Research 16(6) (1999): 876-881.

[54] Andrews, G.P., Laverty, T.P., and Jones, D.S. Mucoadhesive polymeric platforms for controlled drug delivery. <u>European Journal of Pharmaceutics and Biopharmaceutics</u> 71(3) (2009): 505-518.

[55] Pires, C.T.G.V.M.T., Vilela, J.A.P., and Airoldi, C. The Effect of Chitin Alkaline Deacetylation at Different Condition on Particle Properties. <u>Procedia Chemistry</u> 9(0) (2014): 220-225.

[56] Chung, Y., Tsai, C., and Li, C. Preparation and characterization of water-soluble chitosan produced by Maillard reaction. <u>Fisheries Science</u> 72(5) (2006): 1096-1103.

[57] Pacheco, N., et al. Structural Characterization of Chitin and Chitosan Obtained by Biological and Chemical Methods. <u>Biomacromolecules</u> 12(9) (2011): 3285-3290.

[58] Chopra, S., Mahdi, S., Kaur, J., Iqbal, Z., Talegaonkar, S., and Ahmad, F.J. Advances and potential applications of chitosan derivatives as mucoadhesive biomaterials in modern drug delivery. <u>Journal of Pharmacy and Pharmacology</u> 58(8) (2006): 1021-1032.

[59] Filee, P., A. Freichels, C. Jerome, A. Aqil, A. Colige, and T.V. Tchemtchoua. Chitosan biomimetic scaffolds and methods for preparing the same. <u>Google Patents</u> (2011).

[60] Borchard, G., Lueβen, H.L., de Boer, A.G., Verhoef, J.C., Lehr, C.-M., and Junginger, H.E. The potential of mucoadhesive polymers in enhancing intestinal peptide drug absorption. III: Effects of chitosan-glutamate and carbomer on epithelial tight junctions in vitro. <u>Journal of Controlled Release</u> 39(2–3) (1996): 131-138.

[61] Helander, I.M., Nurmiaho-Lassila, E.L., Ahvenainen, R., Rhoades, J., and Roller, S. Chitosan disrupts the barrier properties of the outer membrane of Gram-negative bacteria. <u>International Journal of Food Microbiology</u> 71(2–3) (2001): 235-244.

[62] Rabea, E.I., Badawy, M.E.T., Stevens, C.V., Smagghe, G., and Steurbaut, W. Chitosan as Antimicrobial Agent: Applications and Mode of Action. <u>Biomacromolecules</u> 4(6) (2003): 1457-1465.

[63]   Singla, A.K. and Chawla, M. Chitosan: some pharmaceutical and biological aspects--an update. J Pharm Pharmacol 53(8) (2001): 1047-67.

[64]   Ilium, L. Chitosan and Its Use as a Pharmaceutical Excipient. Pharmaceutical Research 15(9) (1998): 1326-1331.

[65]   Jeon, C. and Ha Park, K. Adsorption and desorption characteristics of mercury(II) ions using aminated chitosan bead. Water Research 39(16) (2005): 3938-3944.

[66]   Yuan, Y., et al. The effect of cross-linking of chitosan microspheres with genipin on protein release. Carbohydrate Polymers 68(3) (2007): 561-567.

[67]   El-Gibaly, I. Development and in vitro evaluation of novel floating chitosan microcapsules for oral use: comparison with non-floating chitosan microspheres. International Journal of Pharmaceutics 249(1–2) (2002): 7-21.

[68]   Sogias, I.A., Williams, A.C., and Khutoryanskiy, V.V. Chitosan-based mucoadhesive tablets for oral delivery of ibuprofen. International Journal of Pharmaceutics 436(1–2) (2012): 602-610.

[69]   Chandy, T. and Sharma, C.P. Chitosan matrix for oral sustained delivery of ampicillin. Biomaterials 14(12) (1993): 939-944.

[70]   Krajewska, B. Diffusion of metal ions through gel chitosan membranes. Reactive and Functional Polymers 47(1) (2001): 37-47.

[71]   Mi, F.-L., Shyu, S.-S., Wu, Y.-B., Lee, S.-T., Shyong, J.-Y., and Huang, R.-N. Fabrication and characterization of a sponge-like asymmetric chitosan membrane as a wound dressing. Biomaterials 22(2) (2001): 165-173.

[72]   Lee, Y.M., et al. The bone regenerative effect of platelet-derived growth factor-BB delivered with a chitosan/tricalcium phosphate sponge carrier. J Periodontol 71(3) (2000): 418-24.

[73]   Huang, M., Khor, E., and Lim, L.-Y. Uptake and Cytotoxicity of Chitosan Molecules and Nanoparticles: Effects of Molecular Weight and Degree of Deacetylation. Pharmaceutical Research 21(2) (2004): 344-353.

[74]   Chen, L., et al. Enhanced nasal mucosal delivery and immunogenicity of anti-caries DNA vaccine through incorporation of anionic liposomes in chitosan/DNA complexes. PLoS One 8(8) (2013): e71953.

[75]   Sajomsang, W., Gonil, P., and Saesoo, S. Synthesis and antibacterial activity of methylated N-(4-N,N-dimethylaminocinnamyl) chitosan chloride. European Polymer Journal 45(8) (2009): 2319-2328.

[76]   Juntapram, K., Praphairaksit, N., Siraleartmukul, K., and Muangsin, N. Synthesis and characterization of chitosan-homocysteine thiolactone as a mucoadhesive polymer. Carbohydrate Polymers 87(4) (2012): 2399-2408.

[77]   Hamman, J.H. and Kotze, A.F. Effect of the type of base and number of reaction steps on the degree of quaternization and molecular weight of N-trimethyl chitosan chloride. Drug Dev Ind Pharm 27(5) (2001): 373-80.

[78]   Mourya, V.K. and Inamdar, N.N. Trimethyl chitosan and its applications in drug delivery. J Mater Sci Mater Med 20(5) (2009): 1057-79.

[79]   Kilcoyne, M., Gerlach, J.Q., Farrell, M.P., Bhavanandan, V.P., and Joshi, L. Periodic acid–Schiff's reagent assay for carbohydrates in a microtiter plate format. Analytical Biochemistry 416(1) (2011): 18-26.

[80]   Pawlak, A. and Mucha, M. Thermogravimetric and FTIR studies of chitosan blends. Thermochimica Acta 396(1–2) (2003): 153-166.

[81]   Kim, C., Choi, J., Chun, H., and Choi, K. Synthesis of chitosan derivatives with quaternary ammonium salt and their antibacterial activity. Polymer Bulletin 38(4) (1997): 387-393.

[82]   Sajomsang, W., Ruktanonchai, U.R., Gonil, P., and Warin, C. Quaternization of N-(3-pyridylmethyl) chitosan derivatives: Effects of the degree of quaternization, molecular weight and ratio of N-methylpyridinium and N,N,N-trimethyl ammonium moieties on bactericidal activity. Carbohydrate Polymers 82(4) (2010): 1143-1152.

[83]   Loubaki, E., Ourevitch, M., and Sicsic, S. Chemical modification of chitosan by glycidyl trimethylammonium chloride. characterization of modified chitosan by 13C- and 1H-NMR spectroscopy. European Polymer Journal 27(3) (1991): 311-317.

[84]   Wang, L.-Y., Gu, Y.-H., Su, Z.-G., and Ma, G.-H. Preparation and improvement of release behavior of chitosan microspheres containing insulin. International Journal of Pharmaceutics 311(1–2) (2006): 187-195.

[85]   Zhang, D., et al. Hybrid Self-Assembly, Crystal, and Fractal Behavior of a Carboxy-Ended Hyperbranched Polyester/Copper Complex. Macromolecular Chemistry and Physics 214(3) (2013): 370-377.

[86]   Cui, H., Webber, M.J., and Stupp, S.I. Self-assembly of peptide amphiphiles: from molecules to nanostructures to biomaterials. Biopolymers 94(1) (2010): 1-18.

[87]   Kokkoli, E., Mardilovich, A., Wedekind, A., Rexeisen, E.L., Garg, A., and Craig, J.A. Self-assembly and applications of biomimetic and bioactive peptide-amphiphiles. Soft Matter 2(12) (2006): 1015-1024.

[88]   Gan, H., et al. Self-assembly of conjugated polymers and ds-oligonucleotides directed fractal-like aggregates. Biomacromolecules 8(5) (2007): 1723-9.

[89]   Huang, Y., Yu, H., Guo, L., and Huang, Q. Structure and Self-Assembly Properties of a New Chitosan-Based Amphiphile. The Journal of Physical Chemistry B 114(23) (2010): 7719-7726.

[90]   Witten, T.A. and Sander, L.M. Diffusion-limited aggregation. Physical Review B 27(9) (1983): 5686-5697.

[91]   Ma, Z., et al. Fractal crystal growth of poly(ethylene oxide) crystals from its amorphous monolayers. Polymer 49(6) (2008): 1629-1634.

[92]   Reches, M. and Gazit, E. Formation of Closed-Cage Nanostructures by Self-Assembly of Aromatic Dipeptides. Nano Letters 4(4) (2004): 581-585.
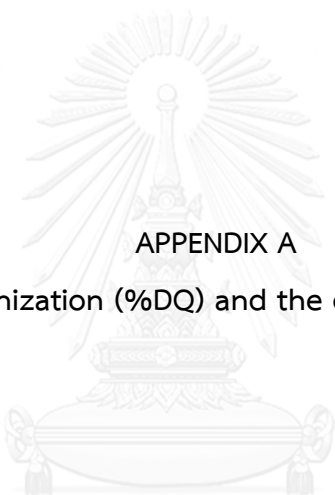
APPENDIX

APPENDIX A

The degree of quaternization (%DQ) and the degree of substitution (%DS)

Determination of the degree of quaternization (%DQ) and the degree of substitution (%DS)

Degree of substitution (%DS)

➢ **Chitin (-NHCOCH₃)**

$$\%DS_{chitin} = \left[\frac{I_{(NHCOCH_3)}}{I_{(H_3-H_6)}} \times \frac{5}{3} \right] \times 100 \quad ......(1)$$

Where, $I_{(NHCOCH_3)}$ is the integral area of GlcNAc protons and $I_{(H_3-H_6)}$ is the integral area of protons at the C3 - C6 carbon of the GluN units.

From ^{1}H NMR spectrum of chitosan (Figure 4.4a)

$$\%DS_{chitin} = \left[\frac{1}{11.39} \times \frac{5}{3} \right] \times 100$$

$$\therefore \quad \%DS_{chitin} = 14.63 \%$$

➢ **Chitosan (-NH₂)**

$$\%DS_{chitosan} = 100 - \%DS_{chitin} \quad ......(2)$$

$$\%DS_{chitosan} = 100 - 14.63$$

$$\therefore \quad \%DS_{chitosan} = 85.37 \%$$

Degree of quaternization (%DQ)

$$\%DQ_{QCS} = \left[\frac{I_{(CH_3)_3}}{I_{(H_3-H_6)}} \times \frac{5}{9}\right] \times 100 \quad ......(3)$$

Where, $I_{(CH_3)_3}$ is the integral area of quaternized amino group protons and $I_{(H_3-H_6)}$ is the integral area of protons at the C3 - C6 carbon of the GluN units.

➤ **TMC-15 (15 mL CH₃I, 15 mL NMP)**

From ^{1}H NMR spectrum of TMC-15 (Figure 4.4b)

$$\%DQ_{TMC} = \left[\frac{1}{2.94} \times \frac{5}{9}\right] \times 100$$

$$\therefore \quad \%DQ_{TMC} = 18.90 \ \%$$

➤ **TMC-30 (30 mL CH₃I, 30 mL NMP)**

From ^{1}H NMR spectrum of TMC-30 (Figure 4.4c)

$$\%DQ_{TMC} = \left[\frac{1}{3.90} \times \frac{5}{9}\right] \times 100$$

$$\therefore \quad \%DQ_{TMC} = 14.25 \ \%$$

➤ **CS Quat-188-1 (1 mL Quat-188)**

From ^{1}H NMR spectrum of CS Quat-188-1 (Figure 4.5d)

$$\%DQ_{CS \ Quat-188} = \left[\frac{1}{2.31} \times \frac{5}{9}\right] \times 100$$

$$\therefore \quad \%DQ_{CS \ Quat-188} = 24.05 \ \%$$

➢ **CS Quat-188-10 (10 mL Quat-188)**

From ^{1}H NMR spectrum of CS Quat-188-10 (Figure 4.5e)

$$\%DQ_{CS\ Quat-188} = \left[\frac{1}{0.90} \times \frac{5}{9} \right] \times 100$$

∴ $\%DQ_{CS\ Quat-188}$ = 61.73 %

➢ **CS Quat-188-20 (20 mL Quat-188)**

From ^{1}H NMR spectrum of CS Quat-188-20 (Figure 4.5f)

$$\%DQ_{CS\ Quat-188} = \left[\frac{1}{0.59} \times \frac{5}{9} \right] \times 100$$

∴ $\%DQ_{CS\ Quat-188}$ = 94.16 %

Degree of 4-CBS substitution (%DS)

$$\%DS_{4-CBS-QCS} = \left[\frac{I_{(SO_2NH_2)}}{I_{(H_3-H_6)}} \times \frac{5}{4} \right] \times 100 \qquad ......(4)$$

Where, $I_{(SO_2NH_2)}$ is the integral area of the benzene ring of 4-CBS-QCS protons and $I_{(H_3-H_6)}$ is the integral area of protons at the C3 - C6 carbon of the GluN units.

➢ **4-CBS-TMC-15 (15 mL CH$_3$I, 15 mL NMP)**

From ^{1}H NMR spectrum of 4-CBS-TMC-15 (Figure 4.6g)

$$\%DS_{4-CBS-TMC} = \left[\frac{1}{12.89} \times \frac{5}{4} \right] \times 100$$

∴ $\%DS_{4-CBS-TMC}$ = 9.70 %

➢ **4-CBS-CS Quat-188-1 (1 mL Quat-188)**

From ^{1}H NMR spectrum of 4-CBS-CSQuat-188-1 (Figure 4.6h)

$$\%DS_{\text{4-CBS-CS Quat-188}} = \left[\frac{1}{12.07} \times \frac{5}{4}\right] \times 100$$

$$\therefore \quad \%DS_{\text{4-CBS-CS Quat-188}} = 10.36 \ \%$$

Degree of 4-CBS substitution (%DS)

$$\%DS_{\text{OA-4-CBS-QCS}} = \left[\frac{I_{(a)}}{I_{(H_3-H_6)}} \times \frac{5}{3}\right] \times 100 \qquad ......(5)$$

Where, $I_{(a)}$ is the integral area of methyl of OA-4-CBS-QCS protons and $I_{(H_3-H_6)}$ is the integral area of protons at the C3 - C6 carbon of the GluN units.

➢ **OA-4-CBS-TMC-15 (15 mL CH$_3$I, 15 mL NMP)**

From ^{1}H NMR spectrum of OA-4-CBS-TMC-15 (Figure 4.6i)

$$\%DS_{\text{OA-4-CBS-TMC}} = \left[\frac{1}{4.88} \times \frac{5}{3}\right] \times 100$$

$$\therefore \quad \%DS_{\text{OA-4-CBS-TMC}} = 34.15 \ \%$$

➢ **OA-4-CBS-CS Quat-188-1 (1 mL Quat-188)**

From ^{1}H NMR spectrum of OA-4-CBS-CSQuat-188-1 (Figure 4.6j)

$$\%DS_{\text{OA-4-CBS-CS Quat-188}} = \left[\frac{1}{4.40} \times \frac{5}{3}\right] \times 100$$

$$\therefore \quad \%DS_{\text{OA-4-CBS-CS Quat-188}} = 37.88 \ \%$$

APPENDIX B

Calibration curve of mucin (type II)

The concentration versus peak absorbance mucin glycoprotein (type II) determined by UV-VIS spectroscopy as the same condition described in chapter III is presented in Table 1B. The plot of calibration curve of mucin is illustrated in Figure 1B and 2B.

Table 1B Absorbance of various concentrations of mucin (type II) at pH 1.2 and 6.4 by UV-VIS spectrometer

| Concentration (mg/2mL)	Absorbance	
	HCl (pH 1.2)	PBS (pH 6.4)
0.2	0.015	0.095
0.4	0.034	0.195
0.6	0.048	0.281
0.8	0.067	0.351
1.0	0.077	0.415
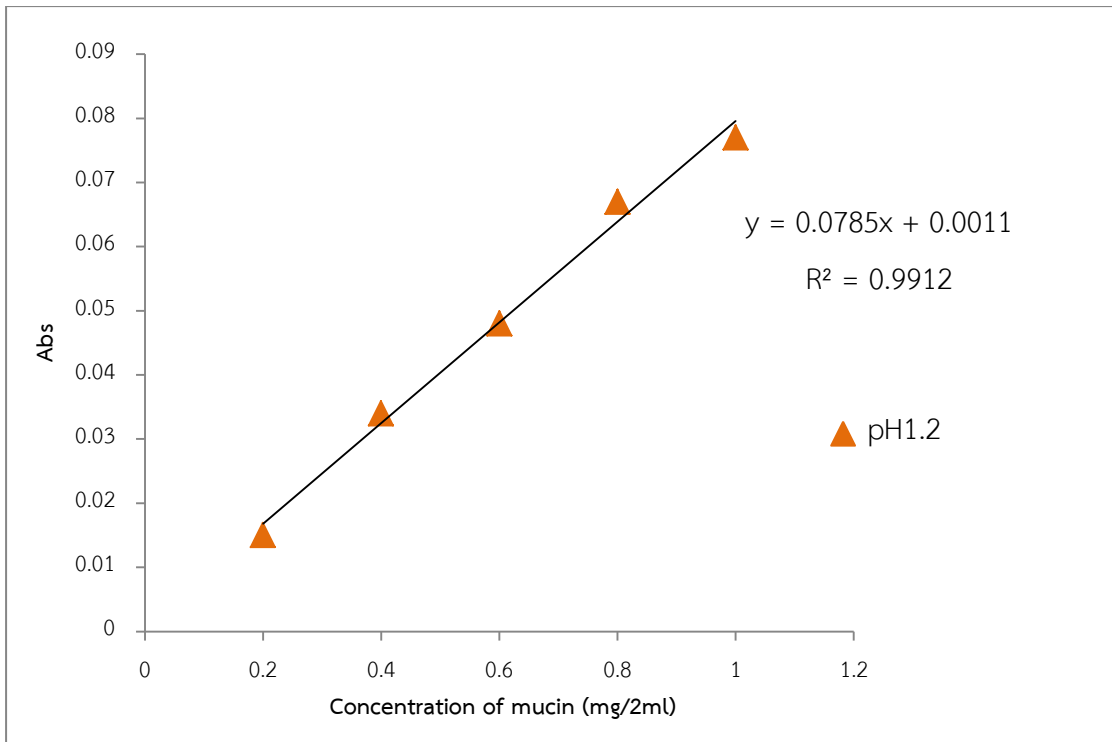
**Figure 1B** Standard curve of mucin at pH 1.2
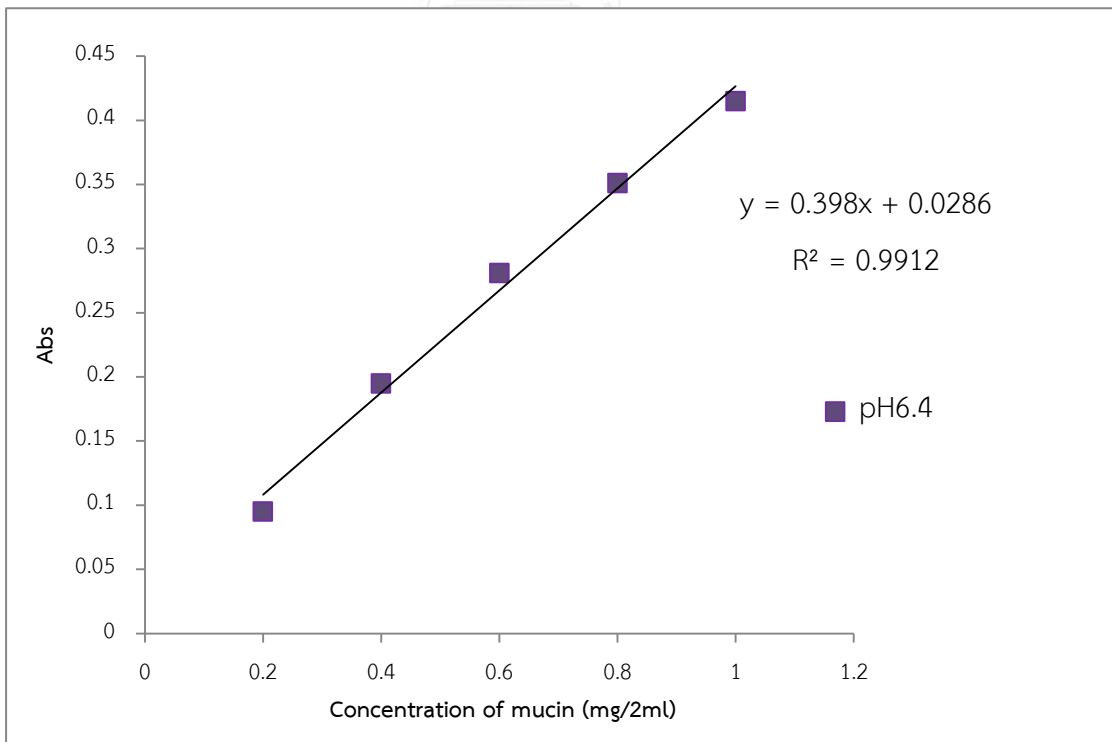
Figure 2B Standard curve of mucin at pH 6.4

Table 2B Absorbed of free and adsorbed of mucin on chitosan and modified chitosan (TMC, CS Quat-188, 4-CBS-TMC, 4-CBS-CS Quat-188, OA-4-CBS-TMC, and OA-4-CBS-CS Quat-188) at pH 1.2 by UV-VIS spectrometer.

Sample	Abs.	Abs.	Abs.	Absorbed of mucin (mg/mL)	SD
Blank	0.072	0.069	0.079	(1-x)/2	
Chitosan	0.153	0.158	0.154	0.111	0.003
TMC	0.149	0.149	0.154	0.124	0.003
4-CBS-TMC	0.148	0.148	0.149	0.149	0.001
OA-4-CBS-TMC	0.125	0.127	0.124	0.289	0.002
CS Quat-188	0.145	0.148	0.149	0.181	0.002
4-CBS-CS Quat-188	0.146	0.149	0.147	0.219	0.002
OA-4-CBS-CS Quat-188	0.125	0.121	0.121	0.339	0.002

Table 3B Absorbed of free and adsorbed of mucin on chitosan and modified chitosan (TMC, CS Quat-188, 4-CBS-TMC, 4-CBS-CS Quat-188, OA-4-CBS-TMC, and OA-4-CBS-CS Quat-188) at pH 6.4 by UV-VIS spectrometer.

Sample	Abs.	Abs.	Abs.	Absorbed of mucin (mg/mL)	SD
Blank	0.080	0.081	0.079	(1-x)/2	
Chitosan	0.394	0.382	0.393	0.216	0.007
TMC	0.381	0.383	0.392	0.240	0.006
4-CBS-TMC	0.396	0.392	0.386	0.255	0.005
OA-4-CBS-TMC	0.306	0.303	0.308	0.319	0.003
CS Quat-188	0.347	0.336	0.337	0.266	0.006
4-CBS-CS Quat-188	0.326	0.327	0.328	0.287	0.001
OA-4-CBS-CS Quat-188	0.311	0.298	0.316	0.389	0.009

VITA

Name : Miss Tanthip Detu-domsut

Date of birth : September 24, 1988

Nationality : Thai

Address : 120 Ratchawithi road, Bang Yi Khan Sub-district, Bang Phlat District, Bangkok 10700

University Education : Bachelor's Degree from Department of Chemistry, Faculty of Science, Mahidol University, 2008-2011

Master's degree from Program of Petrochemistry and Polymer Science, Faculty of Science, Chulalongkorn University, 2012-2014

Conference attendance : Poster presentation "MUCOADHESIVE PROPERTY FOR OLEOYL-4-CARBOXYBENZENESULFONAMIDE-CHITOSAN QUAT-188" The 2014 IUPAC World Polymer Congress "MACRO 2014"